Chapter 15

Signal, Contrast, and Noise

Chapter Contents

Summary: Quantitative methods for understanding the effects of noise in an image are introduced. The important imaging parameter, the signal-to-noise ratio (SNR), is studied in detail. The effects of imaging parameters such as spatial resolution, T_s, and the number of measured data samples N_x, N_y, and N_z on SNR are discussed. Contrast-to-noise ratio (CNR) and visibility concepts are developed as measures of useful information in an image. The issue of SNR as a function of field strength is briefly considered.

Introduction

All physical measurements include either random or systematic noise, which can seriously affect the accuracy or interpretation of a measurement. The degree to which noise affects a measurement is generally characterized by the signal-to-noise ratio (SNR). In MRI, the SNR is a key parameter for determining the effectiveness of any given imaging experiment. If the SNR is not high enough, it becomes impossible to differentiate tissues from one another or the background. Since the signal has already been discussed at some length in previous chapters, a study of the properties of the noise, and development of expressions for SNR

which depend on the imaging parameters are made the major focus of this chapter.[1] SNR as a function of resolution, readout bandwidth (BW_{read}), and imaging time is developed. In MRI, every factor of $\sqrt{2}$ improvement in SNR allows a doubling of resolution in one direction and has an order of magnitude psychological effect on the quality of the image. It is, therefore, necessary to strive in all possible ways to optimize SNR for a fixed spatial resolution.

In Ch. 13, the issue of spatial resolution was studied, and it was determined that MRI can localize signals to very small regions. Localization of the signal is only half of the battle in an MRI experiment. If the signals from different tissues are all the same, a uniform image would be obtained giving no useful anatomic or diagnostic information. The real objective is to localize the signal and be able to differentiate diseased from healthy tissue and one tissue type from another. This implies that there must be a signal difference, referred to as contrast, between different tissues. Combining SNR with contrast leads to the quantity contrast-to-noise ratio (CNR) which is the real 'measure' of the usefulness of an experiment. The second half of this chapter deals with the study of CNR in MRI. It will be found that there are many variables which may be employed to generate contrast in the MRI experiment, and several specific forms of MRI contrast are discussed in depth.

15.1 Signal and Noise

The ability to ascertain whether some object is within a voxel or not depends critically on whether the signal for the object in that voxel can be distinguished from noise. It is the manifestation of the noise in the image, not the noise in the raw data, that is critical here. In this section, the translation from one domain to the other is considered.

15.1.1 The Voxel Signal

The general k-space signal encoding scheme leads to a signal expression (10.2)

$$s(\vec{k}) = \int_V d^3r \rho(\vec{r}) e^{-i2\pi\vec{k}\cdot\vec{r}} \tag{15.1}$$

When the signal expression in (15.1) is written for the 3D Fourier imaging case, it becomes

$$s(k_x, k_y, k_z) = \int\int\int dx\, dy\, dz\, \rho(x, y, z) e^{-i2\pi(k_x x + k_y y + k_z z)} \tag{15.2}$$

As in earlier chapters, the data are assumed to be sampled at a set of points in 3D k-space. These points are separated by Δk_x, Δk_y, and Δk_z, respectively, in the three orthogonal k-space directions, and cover the range defined by the set of integers

$$p',\ q',\ \text{and}\ r' \in (-N_x, N_x - 1), (-N_y, N_y - 1), (-N_z, N_z - 1)$$

The image is reconstructed by applying a discrete inverse Fourier transform to the set of data represented by $s_m(p'\Delta k_x, q'\Delta k_y, r'\Delta k_z)$. Likewise, the image is represented by

[1] Imaging parameters are those variables which are free to be chosen in an experiment, such as T_R, T_E, readout bandwidth, etc., and not the physical constants associated with the sample such as ρ, T_1, or T_2.

$\hat{\rho}_m(p\Delta x, q\Delta y, r\Delta z)$ where p, q, and r typically cover the same range as p', q', and r'. The signal at a given point in the image is

$$\hat{\rho}_m(p\Delta x, q\Delta y, r\Delta z) = \frac{1}{N_x N_y N_z} \sum_{p',q',r'} s(p'\Delta k_x, q'\Delta k_y, r'\Delta k_z) e^{i2\pi\left(\frac{p\,p'}{N_x}+\frac{q\,q'}{N_y}+\frac{r\,r'}{N_z}\right)} \tag{15.3}$$

The effective spin-density $\hat{\rho}_m(p\Delta x, q\Delta y, r\Delta z)$ is also known as the 'voxel signal' $S(\vec{r})$ since it is the signal which will be represented in the volume element $\Delta x\Delta y\Delta z$ at position ($p\Delta x$, $q\Delta y$, $r\Delta z$) in the reconstructed image.[2] Recall that $\hat{\rho}_m(p\Delta x, q\Delta y, r\Delta z)$ often not only represents the transverse magnetization within the voxel volume but also contains a handful of scaling factors and relaxation parameters.[3]

In Secs. 15.1–15.3, it is assumed that voxels are small volumes with uniform spin densities ($\rho(x)$ = a constant). Therefore, all arguments in these sections neglect the possibility of a voxel containing more than one tissue type. Section 15.4 introduces the subject of voxels which are not homogeneous. From Ch. 13, it must also be remembered that the presence of the finite-width point spread function of the discrete Fourier transform (13.17) and the finite blur due to T_2^* decay during sampling (13.57) cause the presence of a nonzero contribution from magnetization outside the voxel boundaries to overlap or contribute to the voxel of interest.

From the discussion on spatial resolution in Ch. 13, the voxel size also represents the area under the point spread function normalized to the zero value of the point spread function. As a result, whenever the spatial resolution is improved by reducing Δx, Δy, or Δz, the total contribution to the voxel signal is reduced proportionately (see, for example, (12.25)); for example, if Δx is halved, $\hat{\rho}_m(p\Delta x, q\Delta y, r\Delta z)$ is also halved. Therefore, in general

$$\hat{\rho}_m(p\Delta x, q\Delta y, r\Delta z) \propto \Delta x\Delta y\Delta z \equiv \text{voxel volume} \equiv V_{voxel} \tag{15.4}$$

The signal limit of (7.20) shows that the peak signal for a homogeneous sample (at $t = 0$ in an FID experiment, or at $t = T_E$ for a 90° gradient echo or spin echo imaging experiment) when transverse signal decay and amplification factors are neglected is given by (7.22)

$$\text{signal for homogeneous object} = \omega_0 M_0 \mathcal{B}_\perp V_{sample} \tag{15.5}$$

where $\mathcal{B}_\perp$ is the transverse field amplitude produced by the receive coil when a unit current is passed through it. Since the voxel is assumed to be a small homogeneous volume element in these discussions, (6.10) can be used to rewrite (15.5) for proton imaging as

$$\begin{aligned} S &\equiv \hat{\rho}_m(p\Delta x, q\Delta y, r\Delta z) \\ &\propto \omega_0 \cdot \frac{\frac{1}{2}\cdot\frac{3}{2}\cdot\gamma^2\hbar^2}{3kT} \cdot B_0 \cdot \mathcal{B}_\perp(p\Delta x, q\Delta y, r\Delta z) \cdot \Delta x\Delta y\Delta z \\ &\propto \frac{\gamma^3\hbar^2}{4kT} \cdot B_0^2 \cdot \mathcal{B}_\perp(p\Delta x, q\Delta y, r\Delta z) \cdot V_{voxel} \end{aligned} \tag{15.6}$$

[2]The reader may recall from Ch. 11 that the Fourier transform of a function represented by a lowercase letter is represented by an uppercase letter. Here lowercase s is used to represent k-space data, $s(\vec{k})$, and an uppercase S is used for the image $S(\vec{r})$, usually when the image voxel signal is being discussed.

[3]The use of effective spin density is no more appropriate than using transverse magnetization or number of spins in a voxel. It has been used in this way because all voxels in a conventional Fourier imaging approach have the same dimensions, and hence, the actual spin density times this volume has the same relative behavior from voxel to voxel as what we have called, for simplicity, effective spin density.

It is important to note the different dependencies in (15.6). Of interest is the direct dependence on the voxel volume, on $\vec{M} \cdot \vec{\mathcal{B}}$ (which is proportional to $\rho_0 \mathcal{B}_\perp$) which is discussed in Secs. 7.3 and 7.4, and on B_0^2, the topic of discussion of a later section in this chapter, as well as the inverse dependence on the sample temperature (which is discussed in Ch. 6).

15.1.2 The Noise in MRI

One of the primary goals of a well-conducted MRI experiment is to obtain enough voxel signal relative to noise (as measured by the ratio of the voxel signal to the noise standard deviation, or signal-to-noise ratio SNR) to observe tissues of interest. Generally, the noise voltage derives from random fluctuations in the receive coil electronics and the sample. Even though there are other sources of signal fluctuations such as digitization noise and pseudo-random ghosting due to moving spins, these sources are minimized in an ideal experiment.

The variance[4] of the fluctuating noise voltage is presented here, without proof,[5] to be

$$\mathrm{var}(emf_{\mathrm{noise}}) \equiv \sigma^2_{thermal} \propto \overline{(emf_{\mathrm{noise}} - \overline{emf_{\mathrm{noise}}})^2} = 4kT \cdot R \cdot BW \tag{15.7}$$

where the horizontal bar over a value implies an average value, R is the effective resistance of the coil loaded by the body, and BW is the bandwidth of the noise-voltage detecting system (in NMR, both the signal and the noise are detected by the receive coil and the bandwidth of reception is determined by the cutoff frequency of the analog low pass filter, BW_{read}).

The proportionality to BW is the principal feature of (15.7), inasmuch as the temperature and resistance of the coils and bodies are not variable. The random thermal fluctuations in the measured signal (as represented in (15.7)) are called 'white' fluctuations because they are characterized by equal expected noise power components at all frequencies within the readout bandwidth.[6] The noise 'variance' of the body and coil together is the sum of variances since these statistical processes are independent, leading to

$$\sigma^2_{thermal}(\vec{k}) = \sigma^2_{body}(\vec{k}) + \sigma^2_{coil}(\vec{k}) + \sigma^2_{electronics}(\vec{k}) \tag{15.8}$$

for all k-space values. For all further subsections, the shorthand notation σ^2_m is typically used in place of $\sigma^2_{thermal}$ where the subscript 'm' connotes 'measured.' It is seen that an effective or total resistance can be inserted into (15.7) representing the sum of the individual components

$$R_{eff} = R_{body} + R_{coil} + R_{electronics} \tag{15.9}$$

15.1.3 Dependence of the Noise on Imaging Parameters

Imaging parameters refer to those factors which can be chosen in an experiment and are not intrinsic properties of the sample. Imaging parameters include factors such as T_E, T_R,

[4] If the probability density function of a random variable x is $f(x)$ so that $\int dx\, f(x) = 1$, the mean of a function $g(x)$ denoted by $\overline{g(x)}$ is given by $\overline{g(x)} = \int dx\, g(x) f(x)$. The variance is defined to be $\mathrm{var}(g(x)) = \int dx f(x)(g(x) - \overline{g(x)})^2$.

[5] For a nice derivation of the Nyquist theorem, see, for example, Kittel in the Suggested Reading. This expression is generally valid up to the order of 10^{14} Hz for protons.

[6] Since white noise has zero mean, the standard deviation is also the square root of the mean of the noise emf squared, i.e., the root mean squared (or rms) value.

Δx, Δy, and Δz, etc., for example, which can be changed in the experiment. The number of spins in the sample, its temperature, and relaxation times are not usually considered imaging parameters. In this section, the effects of relaxation parameters on the experiment are neglected.

Just as the voxel signal depends on the voxel volume which is an imaging parameter, the variance of the voxel signal due to noise is also found to depend on the choice of imaging parameters through the discrete inverse Fourier transform. As before, the measured k-space signal can be thought of as the sum of the true k-space signal $s(k)$ with white noise $\epsilon(k)$ added to it to give the noisy measured signal $s_m(k)$:

$$s_m(k) = s(k) + \epsilon(k) \tag{15.10}$$

For this characterization, the noise autocorrelation function is defined as

$$R_\epsilon(\tau) \equiv \overline{\epsilon(k_p)\epsilon^*(k_q)}|_{\tau \equiv (k_p - k_q)} \tag{15.11}$$

and the Fourier transform of $R_\epsilon(\tau)$, $r_\eta(f)$, is known as the spectral density. $R_\epsilon(\tau)$ is given by an impulse of strength σ_m^2, i.e.,

$$R_\epsilon(\tau) = \sigma_m^2 \delta(\tau) \tag{15.12}$$

and the spectral density is seen to be white since

$$\begin{aligned} r_\eta(f) &\equiv \int d\tau\, R_\epsilon(\tau) e^{-i2\pi f \tau} \\ &= \sigma_m^2 \end{aligned} \tag{15.13}$$

The above expression is valid for continuous k-space data measurement. In the discrete case,

$$\overline{\epsilon(k_p)\epsilon^*(k_q)} = \sigma_m^2 \delta_{pq} \tag{15.14}$$

where now $k_p \equiv p\Delta k$ and $k_q = q\Delta k$ and the Dirac delta is replaced by a Kronecker delta. As before, this implies that any two white noise samples are uncorrelated and the expected noise power is σ_m^2.

White noise is also typically characterized as being Gaussian (or normal) distributed with zero mean and variance σ_m^2. This distribution is denoted by $\mathcal{N}(0, \sigma_m)$. Two Gaussian distributed random variables which are uncorrelated are also independent.

This information makes it possible to evaluate the statistical properties of the noise in the image domain. Using the definition of the discrete inverse Fourier transform acting on $\epsilon(k)$, the white noise transforms to

$$\eta(p\Delta x) = \frac{1}{N} \sum_{p'} \epsilon(p'\Delta k) e^{i2\pi p' \Delta k p \Delta x} \tag{15.15}$$

in the image domain. Recall that the k-space variable $\epsilon(p'\Delta k)$ is assumed to have a distribution of the form $\mathcal{N}(0, \sigma_m)$. Taking the expectation of both sides, we get

$$\begin{aligned} \overline{\eta(p\Delta x)} &= \frac{1}{N} \sum_{p'} \overline{\epsilon(p'\Delta k)} e^{i2\pi p' \Delta k p \Delta x} \\ &= 0 \end{aligned} \tag{15.16}$$

Taking the variance of both sides yields a result independent of p

$$\begin{aligned}\mathrm{var}(\eta(p\Delta x)) \equiv \sigma_0^2(p\Delta x) &= \frac{1}{N^2}\sum_{p'}\sum_{q'}\overline{\epsilon(p'\Delta k)\epsilon^*(q'\Delta k)}e^{i2\pi p\Delta x(p'\Delta k - q'\Delta k)} \\ &= \frac{\sigma_m^2}{N^2}\sum_{p'}\sum_{q'}\delta_{p'q'}e^{i2\pi p\Delta x(p'\Delta k - q'\Delta k)} \\ &= \frac{\sigma_m^2}{N} \qquad (15.17)\end{aligned}$$

where the independence of the random variables $\epsilon(p'\Delta k)$ and $\epsilon(q'\Delta k)$ as defined in (15.14) is used. Note that σ_m^2 is the measured variance of any point in k-space, while σ_0^2 will be used to indicate the noise variance in the image domain. *Hence, the variance measured in any voxel in image space is N times smaller than in the detected signal and is the same for all voxels.* It is also common to quote the noise as the standard deviation $\sigma_0(p\Delta x)$. *In conclusion, from (15.17), as N increases to aN ($a > 1$), $\sigma_0(p\Delta x)$ decreases by the factor $1/\sqrt{a}$.*

The image can now be rewritten, due to the linearity of the Fourier transform, as

$$\hat{\rho}_m(p\Delta x) = \hat{\rho}_{m,0}(p\Delta x) + \eta(p\Delta x) \qquad (15.18)$$

where $\eta(p\Delta x)$ has mean 0 and variance $\sigma_0^2(p\Delta x)$ independent of p. In (15.18), $\hat{\rho}_{m,0}$ represents the pristine image without any noise. As a reminder, the generalization of the expression (15.17) to two dimensions gives

$$\sigma_0^2(p\Delta x)|_{2D} = \frac{\sigma_m^2}{N_x N_y} \qquad (15.19)$$

and to three dimensions gives

$$\sigma_0^2(p\Delta x)|_{3D} = \frac{\sigma_m^2}{N_x N_y N_z} \qquad (15.20)$$

Problem 15.1

Show that $\hat{\rho}(0)$ is nothing more than the average of all k-space data. Hence, rederive (15.17) for the voxel at $p = 0$.

Problem 15.2

In Ch. 13, the partial Fourier imaging problem was presented and the special form of its reconstruction was discussed in detail.

a) Suppose only half the number of k-space lines are collected in the phase encoding direction ($\hat{y}$) to save imaging time (i.e., only one half of k-space is covered). How does this affect the noise in the reconstructed image?

b) Generalize this to the case where n_- points are collected in the negative k_y direction and n_+ points are collected in the positive definite k_y direction (i.e., $k_y \leq 0$).

15.1.4 Improving SNR by Averaging over Multiple Acquisitions

Repeating an entire imaging experiment N_{acq} times[7] and averaging the signal over these N_{acq} measurements to improve the SNR is common practice. The MRI system typically adds the signals directly to one another, and does not store them separately, saving a great deal of data space. The averaged k-space sample $s_{m,av}(k)$ of $s_m(k)$ is:

$$s_{m,av}(k) = \frac{1}{N_{acq}} \sum_{i=1}^{N_{acq}} s_{m,i}(k) \tag{15.21}$$

This implies that

$$\overline{s_{m,av}(k)} = \frac{1}{N_{acq}} \sum_{i=1}^{N_{acq}} \overline{s_{m,i}(k)} = \frac{1}{N_{acq}} \left(N_{acq} s(k)\right) = s(k) \tag{15.22}$$

The noise from each of the N_{acq} acquisitions is assumed to be statistically independent from one acquisition to the next. As a result, the noise variance σ_m^2 from each measurement adds in quadrature to the total noise variance of the averaged signal $s_{m,av}(k)$, i.e.,

$$\begin{aligned} \sigma_{m,av}^2 \equiv \mathrm{var}(s_{m,av}(k)) &= \frac{1}{N_{acq}^2} \sum_{i=1}^{N_{acq}} \mathrm{var}(s_{m,i}(k)) \\ &= \frac{\sigma_m^2(k)}{N_{acq}} \end{aligned} \tag{15.23}$$

Therefore,

$$\sigma_{m,av}(k) = \frac{\sigma_m(k)}{\sqrt{N_{acq}}} \tag{15.24}$$

The SNR of the k-space signal becomes

$$\mathrm{SNR}(k) = \frac{\overline{s_{m,av}(k)}}{\sigma_{m,av}(k)} = \sqrt{N_{acq}} \frac{s(k)}{\sigma_m(k)} \tag{15.25}$$

i.e., *the SNR improves as the square root of the number of acquisitions if the noise is uncorrelated from one experiment to the next.* However, other sources of systematic noise from the MR experiment can lead to σ_m^2 being greater than $\sigma_{thermal}^2$ and these sources will not be reduced the same way by averaging (see Appendix B).

The noise for a given voxel has already been shown to be proportional to σ_m. Hence, the same $\sqrt{N_{acq}}$ dependence carries over into the expression for the SNR/voxel, i.e.,

$$\mathrm{SNR/voxel}(p\Delta x, q\Delta y, r\Delta z) \propto \frac{\sqrt{N_{acq}}}{\sigma_0} \tag{15.26}$$

as well.

[7] These repetitions are sometimes done in consecutive T_R intervals (with the phase encoding gradient(s) at the same value) for minimizing k-space data inconsistencies. In practice, the repetition rate for the acquisition loop is determined by the intended application of the sequence.

Phase Encoding Order When Multiple Acquisitions Are Averaged

Figure 15.1 shows one particular repetition structure for a sequence performing N_{acq} acquisitions before the phase encoding gradient amplitude is augmented. In other applications, this might not be the method of choice for averaging over multiple acquisitions. For example, it is typical in cardiac imaging to actually have the loop structure inside out from the case shown in the figure, i.e., a new acquisition is started after all phase encoding steps have been collected, and the images are averaged finally.

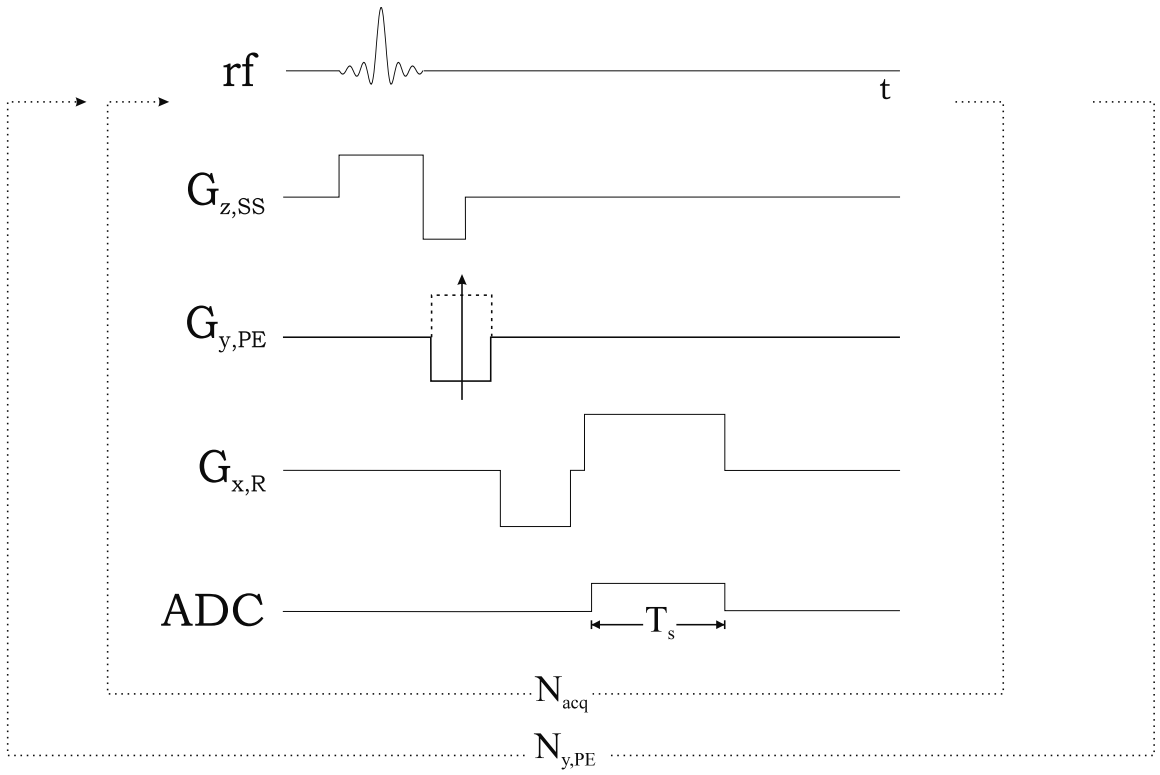

Fig. 15.1: Sequence diagram explicitly demonstrating multiple acquisitions for a 2D FT acquisition method. The phase encoding gradient table is shown in a different form from the usual to remind the reader that the phase encoding gradient is held at one constant value in the acquisition loop. The solid line is supposed to indicate this particular gradient value. The dashed line shows the limit to which the phase encoding gradient is increased at the end of the imaging experiment.

Averaging Unequal Voxel Signals from a Set of Multiple Coils

In MRI, it is becoming increasingly common to use multiple smaller coils to enhance the SNR. Smaller coils pick up less noise than larger coils since they magnetically couple to a smaller volume of the sample. The signal picked up by each coil is used to create individual images which are then combined in some way to create a final image. Unfortunately, these smaller coils, usually lying on the surface of the sample (surface coils), have progressively rapidly weakening B_1 receive fields as a function of distance away from the coil surface.

Therefore, the intensity of images reconstructed from these coils also varies spatially (see Sec. 7.4). In order to construct a final image with reasonable homogeneity of signal and optimal SNR, the images generated by the individual coils must be combined.

Problem 15.3

Suppose that a two-coil system is used such that the voxel signal picked up by coil 1 (S_1) at a point $\vec{x}_a$ equals a, and that picked up by coil 2 (S_2) at the same point equals αa with $\alpha \leq 1$. The standard deviation of the noise associated with either coil is assumed to be the same (say σ_0). Suppose that the two images are added together such that the voxel signal ($\hat{\rho}_m(\vec{x}_a)$) from coil 2 is multiplied by β where β is also ≤ 1.

a) Write an expression for the SNR/voxel after addition of the two weighted voxel signals as a function of β given that the noise distributions in the two coils are statistically independent and are identically equal to each other.

b) Maximize the SNR/voxel as a function of β and show that the SNR is maximized when β equals α.

c) Maximize the SNR/voxel when $\sigma_2 = \beta'\sigma_1$, where β' is a real constant.

From Prob. 15.3, *the optimal linear combination of the two signals is not direct addition as a first guess might suggest. Instead, it is given by the sum-of-squares of the signals picked up by the two coils (the case where β equals α) normalized to the larger of the two signals.* What is the logic behind such a combination? If the two signals are equal, direct addition yields the optimal SNR. However, when one of the two signals is smaller than the other, weighting the smaller measurement by the square of the ratio of the smaller to larger signal produces the optimal SNR. For example, by the time the second signal is one-fifth of the first, there is no need to keep its signal since noise dominates in this case. In this squared sum scheme, the second signal contributes only 4% to the signal, preventing this domination by noise. Recall that the noise picked up by the coil manifests itself as noise with equal variance throughout the image so that, as $\mathcal{B}_\perp$ falls off, the voxel signal decreases while the noise does not.

15.1.5 Measurement of σ_0 and Estimation of SNR

As obtained in (15.19) and (15.20), the standard deviation of the signal in any voxel due to white noise added to the k-space data is independent of voxel number, i.e., the image white noise standard deviation is independent of position in the image. Henceforth, σ_0 and not $\sigma_0(p\Delta x)$ is used to denote the voxel signal standard deviation. In a homogeneous region of a tissue of interest in the image, the average voxel signal over that region is a good estimate of the tissue voxel signal S. In the absence of any systematic variations such as Gibbs ringing, when the SNR in that region is high enough, it is shown later in Sec. 15.7 that the standard deviation in this region is also a very good estimate of σ_0.

A better way to measure σ_0 is to measure the average value or standard deviation of a region-of-interest outside the object where there is no signal (see Fig. 15.2). As shown in Appendix B, the voxel signal here is 'Rayleigh distributed' in the magnitude image. The mean and standard deviation of this random variable are related to the standard deviation of the underlying Gaussian distributed white noise as $1.253\sigma_0$ and $0.665\sigma_0$, respectively. Obtaining σ_0 from either measurement in the background noise gives a more accurate estimate than trying to measure the standard deviation in the image itself (unless the image is perfectly uniform in the region being evaluated). The ratio of the average signal to the estimated value of σ_0 then gives an SNR estimate.

15.2 SNR Dependence on Imaging Parameters

In this section, several imaging parameter dependencies of the SNR on a voxel basis are summarized in different forms. The dependence of SNR/voxel on imaging parameters such as the number of acquisitions N_{acq}, the number of k-space samples N_x, N_y and N_z, the readout bandwidth dependence, and voxel dimensions $\Delta x, \Delta y$ and Δz (or TH in 2D) are discussed in detail. The dependence of SNR on spatial resolution is given utmost importance, and some compromises which have to be kept in mind while improving spatial resolution are presented.

15.2.1 Generalized Dependence of SNR in 3D Imaging on Imaging Parameters

The SNR dependence on imaging parameters is complicated by the noise behavior. Noise depends on many different imaging parameters. From (15.6), (15.7), and (15.19)

$$\text{SNR/voxel} \propto \frac{\Delta x \Delta y \Delta z \sqrt{N_{acq}}}{\sqrt{\frac{BW_{read}}{N_x N_y N_z}}} \tag{15.27}$$

Substituting $\Delta t = \frac{1}{BW_{read}}$ gives

$$\text{SNR/voxel} \propto \Delta x \Delta y \Delta z \sqrt{N_{acq} N_x N_y N_z \Delta t} \tag{15.28}$$

Since $T_s = N_x \Delta t$, substituting this into (15.28) yields

$$\text{SNR/voxel} \propto \Delta x \Delta y \Delta z \sqrt{N_{acq} N_y N_z T_s} \tag{15.29}$$

Equations (15.27)–(15.29) can be rewritten in a number of ways, depending on the parameters which are to be considered. It is necessary to keep in mind that although any parameter in (15.27)–(15.29) may be varied without altering the validity of the relations, the following relations hold

$$\begin{array}{llll} \text{(a)} & L_x = N_x \Delta x & \text{(b)} & L_y = N_y \Delta y \\ \text{(c)} & L_z = N_z \Delta z & \text{(d)} & T_s = N_x \Delta t \\ \text{(e)} & BW_{read} = \frac{1}{\Delta t} = \gamma G_x L_x & \text{(f)} & BW/\text{voxel} = BW_{read}/N_x \end{array} \tag{15.30}$$

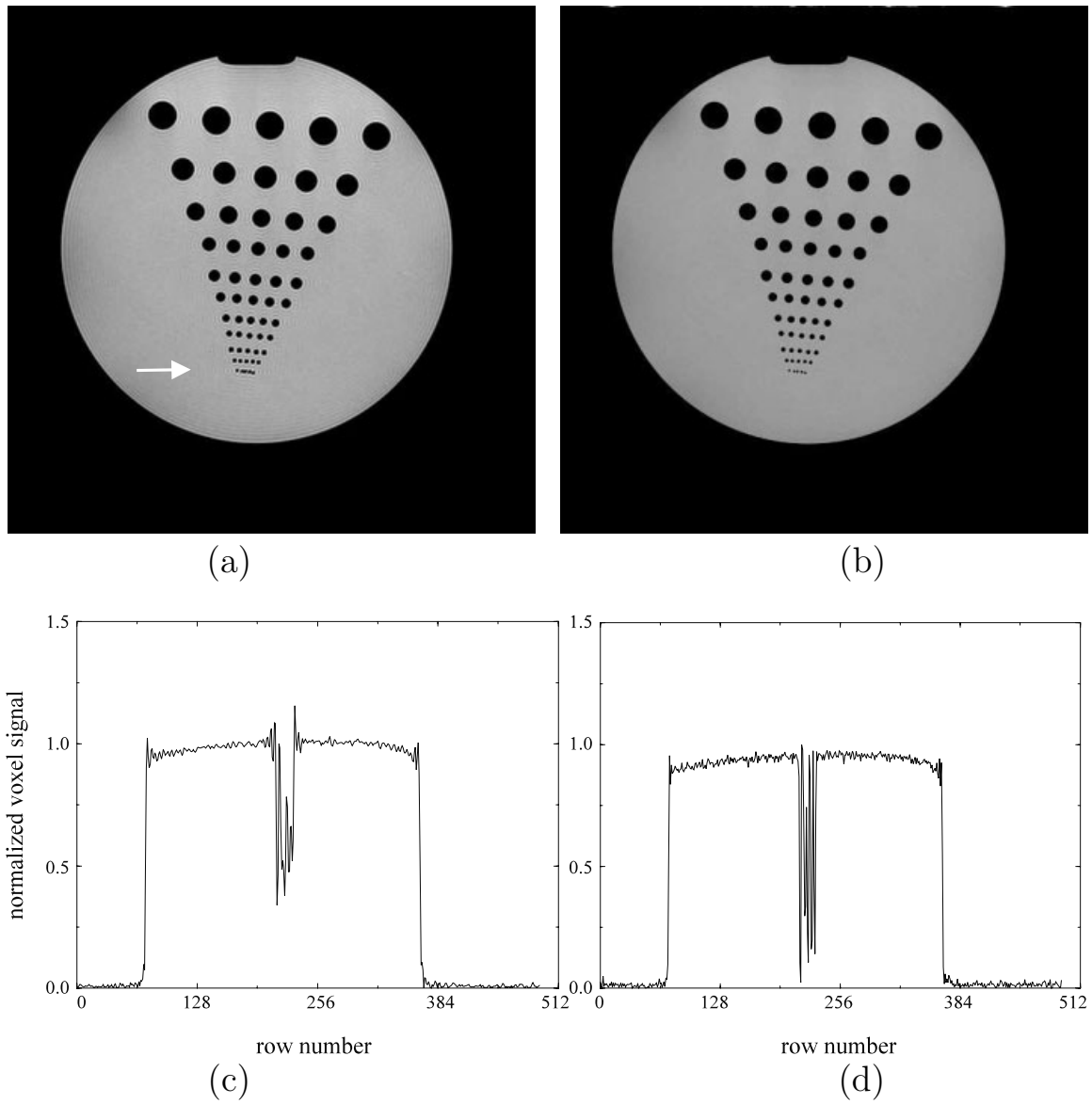

Fig. 15.2: Two images collected with identical T_R, T_E, and G_x. However, N_x, N_y, and T_s in (b) are two times the same values in (a), leading to an improvement in spatial resolution. This increase in resolution leads to a reduction of the SNR by a factor of 2. Noise standard deviation inside the object is estimated by taking $1/1.253 \simeq 0.8$ times the mean measured in a region outside the phantom where there is no signal (see Appendix B). This noise-only region has to lie reasonably away from the edge of the object, and there should be no artifacts nearby. The profiles in (c) and (d) illustrate the larger variation in noise for (a) versus (b), respectively. They also show the higher resolution associated with (d), where five distinct dips (each corresponding to one resolution element) are visible versus only three in (c). The profiles were taken through the row cutting through the last row of smallest resolution elements.

These interrelations exist implicitly in each of the above expressions for the SNR. Therefore, whenever a parameter in a given expression for SNR is varied, the resultant effects on the rest of the parameters must be checked. Also, it is obvious that through these relations a number of other expressions for the SNR may be developed to highlight the effects of varying a certain subset of these parameters. Often an expression for SNR will be accompanied by a condition that some quantity be kept constant which limits how certain parameters may be varied. Finally, there are other dependencies of the signal related to data acquisition and tissue properties, which will be dealt with in Sec. 15.4.

To calculate what happens in the case of a fixed variable, an implicit form can be substituted into (15.29). For example, since $\Delta x = L_x/N_x$, if Δx is fixed, L_x and N_x cannot vary arbitrarily and (15.28) or (15.29) are better written as

$$\text{SNR/voxel} \propto L_x \Delta y \Delta z \sqrt{\frac{N_y N_z \Delta t}{N_x}}\Bigg|_{\Delta x = L_x/N_x = constant} \tag{15.31}$$

Other such specialized proportionalities can be derived.

An increase in the spatial resolution by a factor of 2 in both in-plane directions leads to a factor of 2 loss in SNR when the increased spatial resolution is achieved by maintaining the read gradient fixed while T_s is doubled (from (15.29)). Such an example is shown in Fig. 15.2, from which the mean and standard deviation estimates were obtained. Taking the ratio of the mean of the local background to the noise standard deviation in the two cases demonstrates the consistency of the measured SNR with that expected from (15.29). Doing this in a region where the profile is flat yields an SNR/voxel of 187.5 for Fig. 15.2a and 91.0 for Fig. 15.2b.

15.2.2 SNR Dependence on Read Direction Parameters

From (15.29), with all other parameters maintained constant, the SNR dependence on read direction parameters can be reduced to

$$\text{SNR/voxel}|_{read} \propto \Delta x \sqrt{T_s} \tag{15.32}$$

Although (15.32) depends only upon two parameters, dependencies on L_x, BW, etc. are implicit in this expression (see (15.29) and (15.30)). Due to the importance of understanding the effects of altering read direction parameters, several example situations are shown in Table 15.1. Case 1 is chosen as a reference and given an SNR of unity. Also, note that in order to simplify the treatment, all of the situations in Table 15.1 are restricted to doubling or halving the parameters involved. There are also practical aspects to these choices, which will be discussed below.

From (15.32), it appears that it might be possible to obtain very high resolution without reducing SNR by shrinking Δx while increasing T_s. Realistically, however, there is a limit to how long T_s can be before the signal is seriously degraded by T_2^* effects.

Oversampling to Avoid Aliasing

Although the topic of aliasing has been dealt with in Ch. 12, it is useful here to revisit it in terms of how changing the FOV affects the SNR in a given experiment. In Table 15.1, cases

Case	Δx	N_x	L_x	G_x	Δt	T_s	SNR
Reference case							
1	Δx_0	N_0	L_0	G_0	Δt_0	$T_{s,0}$	1
Data reduction and oversampling							
2	Δx_0	$N_0/2$	$L_0/2$	G_0	$2\Delta t_0$	$T_{s,0}$	1
3	Δx_0	$2N_0$	$2L_0$	G_0	$\Delta t_0/2$	$T_{s,0}$	1
Degrading spatial resolution							
4	$2\Delta x_0$	$N_0/2$	L_0	G_0	Δt_0	$T_{s,0}/2$	$\sqrt{2}$
5	$2\Delta x_0$	$N_0/2$	L_0	$G_0/2$	$2\Delta t_0$	$T_{s,0}$	2
Improving spatial resolution							
6	$\Delta x_0/2$	N_0	$L_0/2$	G_0	$2\Delta t_0$	$2T_{s,0}$	$1/\sqrt{2}$
7	$\Delta x_0/2$	N_0	$L_0/2$	$2G_0$	Δt_0	$T_{s,0}$	1/2
8	$\Delta x_0/2$	$2N_0$	L_0	$2G_0$	$\Delta t_0/2$	$T_{s,0}$	1/2
9	$\Delta x_0/2$	$2N_0$	L_0	G_0	Δt_0	$2T_{s,0}$	$1/\sqrt{2}$

Table 15.1: Table showing the SNR/voxel when the voxel size is changed in the read direction under different conditions. The SNR/voxel is given relative to that of case 1 and can be seen to correlate exactly with $\Delta x(T_s)^{1/2}$ or equivalently, $(\Delta x/G_x)^{1/2}$. Note that T_s and G_x vary similarly from baseline conditions in the different cases.

2 and 3 demonstrate that altering the FOV does not alter the SNR of an experiment as long as T_s and Δx are unchanged. There are two important implications of this result.

First, it is possible to avoid aliasing in a given experiment by doubling the FOV in the read direction. This is accomplished by collecting twice as many points without varying the read gradient G_x or T_s (referred to as oversampling (case 3)), which neither degrades nor improves the SNR of the experiment. Therefore, *in many practical imaging situations, oversampling is used to double the FOV in the read direction and reduce aliasing artifacts without sacrificing SNR or lengthening T_s or the acquisition time.* Consider acquiring a transverse image of the human chest, for example, where the left to right dimension of the experiment is very large and is most likely to be chosen as the read direction. Oversampling in the read direction is then used to guarantee that the FOV extends past the patient's arms without increasing imaging time, or degrading SNR.

Alternatively, for a small object, where aliasing is not a problem and data storage space is at a premium, choosing a smaller FOV and collecting fewer data points (case 2) does not reduce SNR.

Degrading Resolution to Increase SNR

In case 4, Δx is increased by a factor of 2, the number of data points collected is halved and T_s is also halved. As seen from Table 15.1, SNR is increased by $\sqrt{2}$. If lower resolution can be tolerated, this increase in SNR could lead to better tissue recognition, and the reduction in T_s could be beneficial in reducing the chemical shift artifact (discussed in detail in Ch. 17), in overcoming static field inhomogeneity effects (since BW/voxel is increased), and in reducing relaxation effects during sampling.

In case 5, resolution is reduced by a factor of 2, and SNR is doubled because this increase in resolution is achieved while T_s is held constant. A doubling of SNR is a significant SNR improvement. Note that this effect is achieved by reducing the read gradient by a factor of 2. In most cases, reducing the gradient is not a problem, but it must be kept in mind that if the applied gradient strength reduces to a level comparable to those produced by local field inhomogeneities, then severe image distortion will result (as detailed in Ch. 20). *This trick of using a fixed T_s with the read gradient halved to acquire low resolution images and obtain a factor of 2 improvement in SNR is commonly used in clinical applications.*

Improving Resolution in the Read Direction

In both cases 6 and 7, Δx is halved by reducing the FOV by a factor of 2 without changing the number of sampled points. This should be done only if the FOV in case 1 is greater than or equal to twice the width of the object in the read direction so that aliasing will be avoided. In case 6, T_s is doubled by doubling Δt. This method leads to a reduction of SNR of only $\sqrt{2}$ since BW/voxel is again halved. Realistically, T_s must be short enough in case 1 so that, when it is doubled, it is still much shorter than T_2^*. In case 7, L_x is halved by doubling the read gradient G_x. This approach requires that enough gradient power be available to double G_0. Unfortunately, SNR is reduced by a factor of 2, making this a very inefficient approach. In case 8, Δx is halved by doubling N_x and keeping L_x and T_s fixed, which requires doubling G_x and halving Δt_0. This also leads to a halving of the SNR. In case 9, Δx is halved by

doubling N_x while keeping both L_x and G_x fixed. This requires doubling the total sampling time, but is accompanied by only a $\sqrt{2}$ reduction in SNR. This is probably the optimal way to double the resolution of the experiment as long as the increased T_s is not comparable to T_2^*, and storing the extra data is not a problem, although it is similar to case 6 which requires less storage space but a smaller object.

Problem 15.4

A better understanding and feel for the SNR variation in the read direction can be obtained by relating the SNR to a combination of Δx and the BW/voxel.

a) Show that SNR/voxel $\propto \Delta x/\sqrt{BW/\text{voxel}}$.

b) When Δx is halved with a corresponding doubling of G_x (as in cases 7 and 8 in Table 15.1), how does BW/voxel vary in these two cases? What happens to the voxel signal? What happens to the SNR/voxel? Does the FOV change?

c) When Δx is halved by increasing N_x without a corresponding doubling of G_x (as in case 9 in Table 15.1), how does BW/voxel vary? What happens to the voxel signal and the SNR/voxel?

d) Find two other ways to halve Δx of the experiment depicted in Table 15.1. Hint: See cases 6 through 9.

e) Given the following parameters, find Δx_0 and the proportional SNR/voxel as given in (15.32). $\text{FOV}_{read} = 256$ mm, $N_x = 256$, $G_x = 2.5\,\text{mT/m}$, $G_{max} = 15\,\text{mT/m}$, with the T_2^* of the tissue of interest being 20 ms. Assume that you would like to reduce Δx_0 in this case to $\Delta x_0/2$. Discuss how you might best accomplish this in terms of getting optimal SNR/voxel. For deriving this result, assume that T_s has to be less than or equal to T_2^*.

Since T_s equals $1/(\gamma G_x \Delta x)$, the proportionality in (15.32) can be rewritten as

$$\begin{aligned} \text{SNR/voxel} &\propto \sqrt{\frac{\Delta x}{G_x}} \\ &\propto \Delta x\sqrt{T_s} \end{aligned} \tag{15.33}$$

Either expression contains no hidden dependencies and requires none of the imaging parameters to be fixed, i.e., they can be applied to any situation for computing the relative SNR change. According to this expression, the SNR/voxel decreases only by a factor of $\sqrt{2}$ for every halving of Δx as long as the read gradient is fixed. SNR however reduces by a factor of 2 if this improvement in spatial resolution is accompanied by a doubling of G_x. Note consistency with these observations for cases 6 through 9 in Table 15.1. The only way to improve the SNR when Δx is made smaller is to increase T_s accordingly. Unfortunately, this is possible only up to a point, either before relaxation effects begin to reduce the k-space signal or before T_s starts to limit the minimum T_R value. The features in cases 6 through 9 are also summarized in Fig. 15.3.

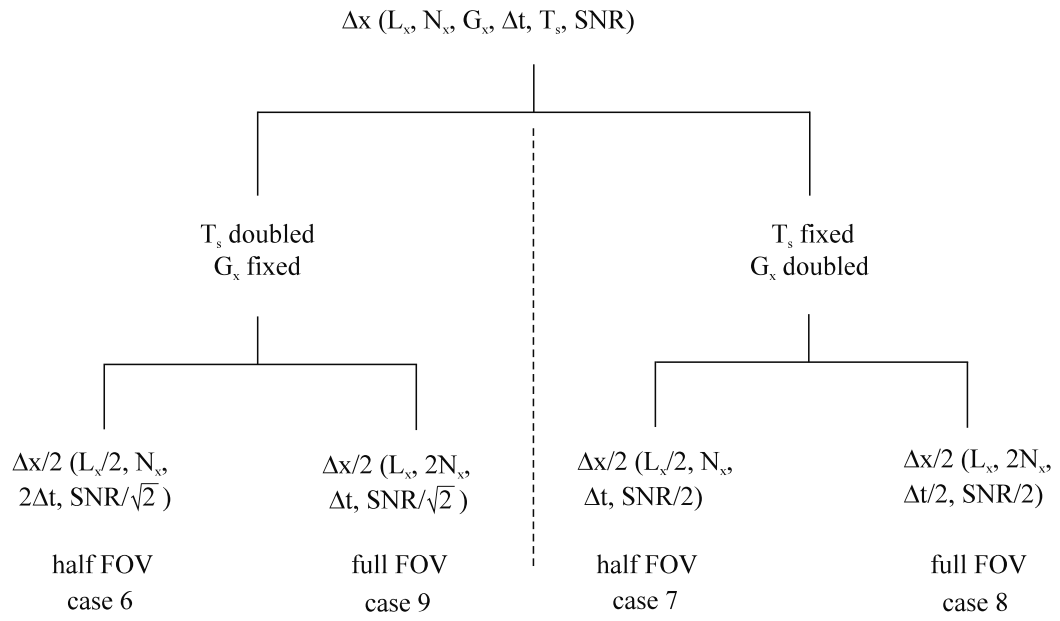

Fig. 15.3: Different ways of achieving improved spatial resolution in the read direction, and their effects on SNR. This figure summarizes cases 6 through 9 in Table 15.1, showing also what parameters were changed in comparison with case 1 to attain high resolution. For T_s fixed, either approach yields a loss of 2 in SNR while for T_s doubled, only a loss of square root of 2 in SNR occurs.

15.2.3 SNR Dependence on Phase Encoding Parameters

Pulling out just the SNR dependence on parameters which change only the image characteristics in the in-plane and through-plane phase encoding directions ($\hat{y}$ and $\hat{z}$, respectively) gives

$$\text{SNR/voxel} \propto \Delta y \Delta z \sqrt{N_y N_z} \tag{15.34}$$

(recall $L_y = N_y \Delta y$ and $L_z = N_z \Delta z$). *There are only two alternate methods for improving spatial resolution in the phase encoding directions: first, decreasing Δy or Δz by increasing N_y or N_z while keeping L_y or L_z fixed* (case 3 in Table 15.2), *or second, decreasing Δy or Δz by decreasing L_y or L_z while keeping N_y or N_z fixed* (case 2 in Table 15.2).

Consider halving Δy using either of these methods. In the first method, the SNR decreases only by a factor of $\sqrt{2}$, whereas in the second method, the SNR decreases by a factor of 2. What are the advantages or disadvantages of either method? The first method, requiring doubling N_y, takes twice as long to complete compared to the second method. If the SNR is good enough and aliasing is avoided, the second method is twice as time-efficient as the first while having $\sqrt{2}$ worse SNR in comparison with the first. Of course, in the same imaging time as required by the first method, two acquisitions can be performed with the second method to reclaim the factor of $\sqrt{2}$ SNR loss, while maintaining the advantage of requiring less image storage space. These two cases are highlighted in Table 15.2.

Case	Δy	N_y	L_y	$G_{y,max}$	T_T	SNR
Reference case						
1	Δy_0	$N_{y,0}$	$L_{y,0}$	$G_{y,0}$	T_{T_0}	1
Improved spatial resolution						
2	$\Delta y_0/2$	$N_{y,0}$	$L_{y,0}/2$	$2G_{y,0}$	T_{T_0}	$1/2$
3	$\Delta y_0/2$	$2N_{y,0}$	$L_{y,0}$	$2G_{y,0}$	$2T_{T_0}$	$1/\sqrt{2}$

Table 15.2: Two different ways to improve spatial resolution in the phase encoding direction, and their effects on the SNR and total imaging time.

15.2.4 SNR in 2D Imaging

The SNR expression in (15.29) can be rewritten for a 2D imaging experiment. The voxel now has dimensions of $\Delta x \times \Delta y \times TH$. Also, N_z is replaced by unity. Therefore

$$(\text{SNR/voxel})|_{2D} \propto \Delta x \Delta y TH \sqrt{N_y T_s} \tag{15.35}$$

In other words, a 2D imaging experiment performed with exactly the same imaging parameters (including T_R, T_E, and flip angle) with $TH = \Delta z$ has $\sqrt{N_z}$ worse SNR in comparison with the 3D imaging experiment. However, the 2D imaging experiment requires an imaging time which is N_z times shorter than the 3D experiment. However, it is typically possible to collect the data for only one slice per T_R when the T_R value in the 2D imaging experiment equals the practically sensible choice of short T_R in the 3D imaging experiment. To obtain the same spatial coverage in the slice select direction requires N_z imaging experiments, increasing the total imaging time by N_z in the 2D imaging case. If the same imaging time is used for both the 2D and 3D imaging experiments, the same volume of coverage and the same contrast as the 3D can be achieved in 2D imaging albeit only with $\sqrt{N_z}$ less SNR. Or a single slice with the same SNR as the 3D experiment (obtained by imaging with $N_{acq_{2D}} = N_z$) can be obtained. The most efficient means of collecting 2D data and covering the same region-of-interest as in the 3D imaging case is to use $T_{R_{2D}} = N_z T_{R_{3D}}$ and use a multi-slice acquisition[8] (although this guarantees neither that the 2D SNR is as good as the 3D SNR as discussed below nor that the contrast is comparable with the 3D imaging method).

[8]See Ch. 10 for more details.

15.2.5 Imaging Efficiency

In clinical applications, patient comfort and patient throughput are important day-to-day issues. The longer the imaging time per patient, the more patient discomfort and the less throughput. In Fourier imaging, the total imaging time for each imaging experiment is dependent directly on the number of sequence cycle repetitions. Consider the 3D imaging case, where the total imaging time is given by

$$T_T = N_{acq} N_y N_z T_R \tag{15.36}$$

The general wisdom is that, since

$$(\text{SNR/voxel})_{3D} \propto \Delta y \Delta z \sqrt{N_y N_z} \tag{15.37}$$

with L_y and L_z constant, if either N_y or N_z is halved and consequently Δy or Δz is doubled, respectively, not only is the SNR improved by a factor of $\sqrt{2}$, but the imaging time is also halved. As a consequence, if the same imaging time as that for the better resolution scan is used, the SNR can be improved further by an additional factor of $\sqrt{2}$ by averaging 2 acquisitions at lower resolution. Thereby, the SNR-per-unit-time is doubled in comparison with the high resolution image. *A time-normalized SNR is therefore considered a measure of imaging efficiency.* The normalization to time is done not on a per-unit-time basis, but on a per square root of time basis, since, for a fixed T_R, SNR is proportional to $\sqrt{T_T} = \sqrt{N_{acq} N_y N_z T_R}$. Therefore, for a fixed T_R, the imaging efficiency is defined as

$$\begin{aligned} \Upsilon \equiv \frac{(\text{SNR/voxel})_{3D}}{\sqrt{T_T}} &\propto \frac{\Delta x \Delta y \Delta z \sqrt{N_{acq} N_y N_z T_s}}{\sqrt{N_{acq} N_y N_z}} \\ &\propto \Delta x \Delta y \Delta z \sqrt{T_s} \end{aligned} \tag{15.38}$$

In other words, an image with better spatial resolution, such as with Δy or Δz halved, is considered only half as SNR-efficient as an image acquired with voxel size Δy or Δz, respectively. Again, this measure does not include the role of voxel size relative to object size. The main conclusion is that high resolution can be achieved efficiently only in the read direction, and even that is limited by the need to keep T_s on the order of T_2^* or less.

15.3 Contrast, Contrast-to-Noise, and Visibility

Even the highest signal-to-noise ratio does not guarantee a useful image. An important aim of imaging for diagnostic purposes is to be able to distinguish between diseased and neighboring normal tissues. If the imaging method used does not have a signal-manipulating mechanism which produces different signals for the two tissues, distinguishing the two tissues is not possible. MRI is blessed with an abundance of signal-manipulating mechanisms, as the signal is dependent on a wide variety of tissue parameters. The problem of distinguishing a given (diseased) structure from surrounding (normal) tissue in the presence of added white noise falls under the broad category of the 'signal detection' problem, and requires an understanding of the importance of Contrast-to-Noise Ratio (CNR).

15.3.1 Contrast and Contrast-to-Noise Ratio

The common way to look at this problem is to examine the absolute difference in the signal between the two tissues of interest. If these tissues are labeled A and B, their signal difference[9] is defined as the 'contrast:'

$$C_{AB} \equiv S_A - S_B \tag{15.39}$$

where S_A and S_B are the voxel signals from tissues A and B, respectively. Although the inherent contrast may be large enough to detect a change, if the noise is too large, the signal difference would not be visible to the eye or to a simple signal difference threshold algorithm. The more appropriate measure is the ratio of the contrast to the noise standard deviation[10] known as the contrast-to-noise ratio, CNR:

$$\mathrm{CNR}_{AB} \equiv \frac{C_{AB}}{\sigma_0} = \frac{S_A - S_B}{\sigma_0} = \mathrm{SNR}_A - \mathrm{SNR}_B \tag{15.40}$$

The utility of this definition is best illustrated with a simple statistics discussion. For Gaussian distributed white noise, the probability that two tissues are different if CNR_{AB} equals $2\sqrt{2}$ is 95% and if CNR_{AB} equals $3\sqrt{2}$ is 99%. Ideally we would like to design the MR experiment to have sufficient spatial resolution to resolve the two tissues of interest (such as gray matter and white matter) and to have a high enough CNR that they can be distinguished from each other.

15.3.2 Object Visibility and the Rose Criterion

If multiple independent signal measurements N_{acq} are performed, an average of these signal measurements implies that the effective noise standard deviation becomes

$$\sigma_{eff} = \frac{\sigma_0}{\sqrt{N_{acq}}} \tag{15.41}$$

In an image where tissue A occupies n_{voxel} voxels, each of which has signal S_A with independent additive white noise with standard deviation σ_0, a similar voxel-averaging scenario can be incorporated into the detection criterion (with N_{acq} replaced by n_{voxel}) via a new measure referred to as the 'object visibility' or

$$\mathcal{V}_{AB} \equiv \frac{C_{AB}}{\sigma_{eff}} = \frac{C_{AB}}{\sigma_0}\sqrt{n_{voxel}} = \mathrm{CNR}_{AB}\sqrt{n_{voxel}} \tag{15.42}$$

Again, the noise in each voxel of the image, σ_0, is assumed to be the same for both tissues.

[9] It is also common to refer to contrast as C_{AB}/S_A or C_{AB}/S_B. We define these as relative contrast ratios.

[10] Since no physical subtraction is performed in the image, the standard deviation used is that common to both tissues A and B, i.e., σ_0. If a contrast image were created, then σ_0 would be replaced by $\sqrt{2}\sigma_0$.

The Rose Criterion

The visibility threshold can be determined empirically. Based on experiments with human observers detecting circular objects shone on a television screen, Rose found that random fluctuations in the photon flux forming the object confused the observer, and a minimum 'SNR' was required for confident object detection. Depending on the observer's expertise and what is being observed, a detection SNR threshold varying between 3 and 5 was found to be required for object recognition. This requirement is known as the 'Rose Criterion' in the diagnostic imaging literature.

A visibility threshold of about 4 can be reinterpreted for the tissue discrimination problem as follows: a Gaussian model for the additive white noise is found to be a rather good approximation for the thermal noise. With this assumption made, the image signal from tissues A and B can be modeled by two Gaussian distributions centered at S_A and S_B, respectively, with the same standard deviation σ_0. Now, if $(S_A - S_B) = 4\sigma_0$, as it would be for single-voxel tissues A and B, the two Gaussian distributions are separated by $4\sigma_0$ (see Fig. 15.4). Since a distance $2\sigma_0$ to one side of the mean covers about 97.5% of the area under a Gaussian distribution, it is reasonable to expect the human observer to choose a threshold which is $2\sigma_0$ away from either S_A or S_B. Then, the probability of the observer incorrectly classifying a voxel as belonging to one or the other tissue is 0.025, i.e., this is a 1-in-40 chance occurrence. That is, the probability of detection of the tissue is very high: for a multi-voxel object when $\mathcal{V}$ equals 4, only 1 in 40 voxels in the object will be classified incorrectly by the observer as a background voxel, and vice versa; for a single-voxel object, there is only a 1-in-40 chance of not detecting it.[11] This description is essentially a rule of thumb, as the perception of the object is likely to be much more complicated.

Problem 15.5

---

a) Show for cases 6 and 9 of Table 15.1 that $\mathcal{V}$ remains constant for a multi-voxel object.

b) It has been suggested that the Great Wall of China can be seen as the only man-made structure visible from outer space, yet it is only a few meters wide. Postulate why this might be possible based upon a visibility argument.

The effect of object size, σ_0, and contrast level on object visibility can be visually demonstrated to be determined by the quantity $\mathcal{V}$ as it was defined in (15.42) by observing the images in Fig. 15.5. The model image with no noise added is shown in Fig. 15.5a. The simulated objects are disk-like objects of linearly decreasing radius (one voxel radius to five voxel radius) going from top to bottom and linearly increasing signal values going from left to right (doubling from column 1 to column 5; actual values can be computed from SNR values quoted in the caption for Fig. 15.5) imaged in a zero signal background. The model image

[11] As for footnote 10, visibility has been defined relative to σ_0, not $\sqrt{2}\sigma_0$. If the latter were chosen, the above argument is still valid but the quoted visibility in the case being considered would be $2\sqrt{2}$ rather than 4.

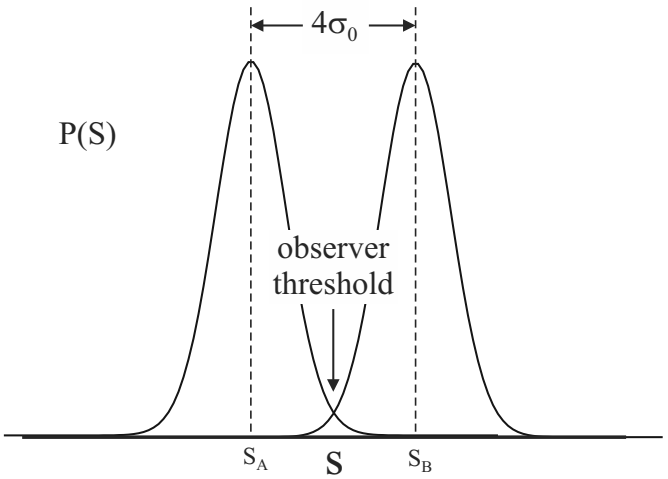

Fig. 15.4: Image signal distribution of two tissues A and B with added Gaussian distributed white noise. When $(S_A - S_B)$ equals $4\sigma_0$, the probability of an error in the detection of tissue A is about 0.025 when a threshold of $2\sigma_0$ is used. Likewise, the probability of mis-classifying a noise point as an object is also 0.025.

is assumed to be all real, whereas the noise is assumed to have uncorrelated and equal expected power in both the real and imaginary image channels. The noisy images were created by adding the real channel noise to the model and taking the magnitude of the two image channels after this addition. As described in the earlier discussion, the smaller disks become indistinguishable from noise at the lower SNR levels while the larger disks are detectable even at degraded SNR levels. Also, the higher the true contrast of the object, the higher the SNR degradation must be before such an object becomes undetectable. It is easy to note that at a given SNR level (images at different SNR levels are shown in Figs. 15.5b–15.5d), an imaginary diagonal line can be drawn separating the barely detectable objects from the undetectable objects and the clearly detectable objects. It is found that the objects along such a diagonal line have a constant value of the product of the signal with the square root of the number of voxels occupied by the object. This shows that the threshold of visibility is determined by the quantity $\mathcal{V}$ defined in (15.42).

15.4 Contrast Mechanisms in MRI and Contrast Maximization

As mentioned earlier, MRI has the flexibility to manipulate the tissue signal in many ways, leading to numerous contrast mechanisms. The flexibility arises from the MR signal dependence on many imaging parameters and tissue parameters. The most basic contrast generating mechanisms are based on spin density, and T_1 and T_2 differences between tissues. Others are flow, magnetic susceptibility differences, magnetization transfer contrast, tissue saturation methods, contrast enhancing agents and diffusion, all of which are discussed in one place or another in later chapters of this book. In this section, the focus is on three

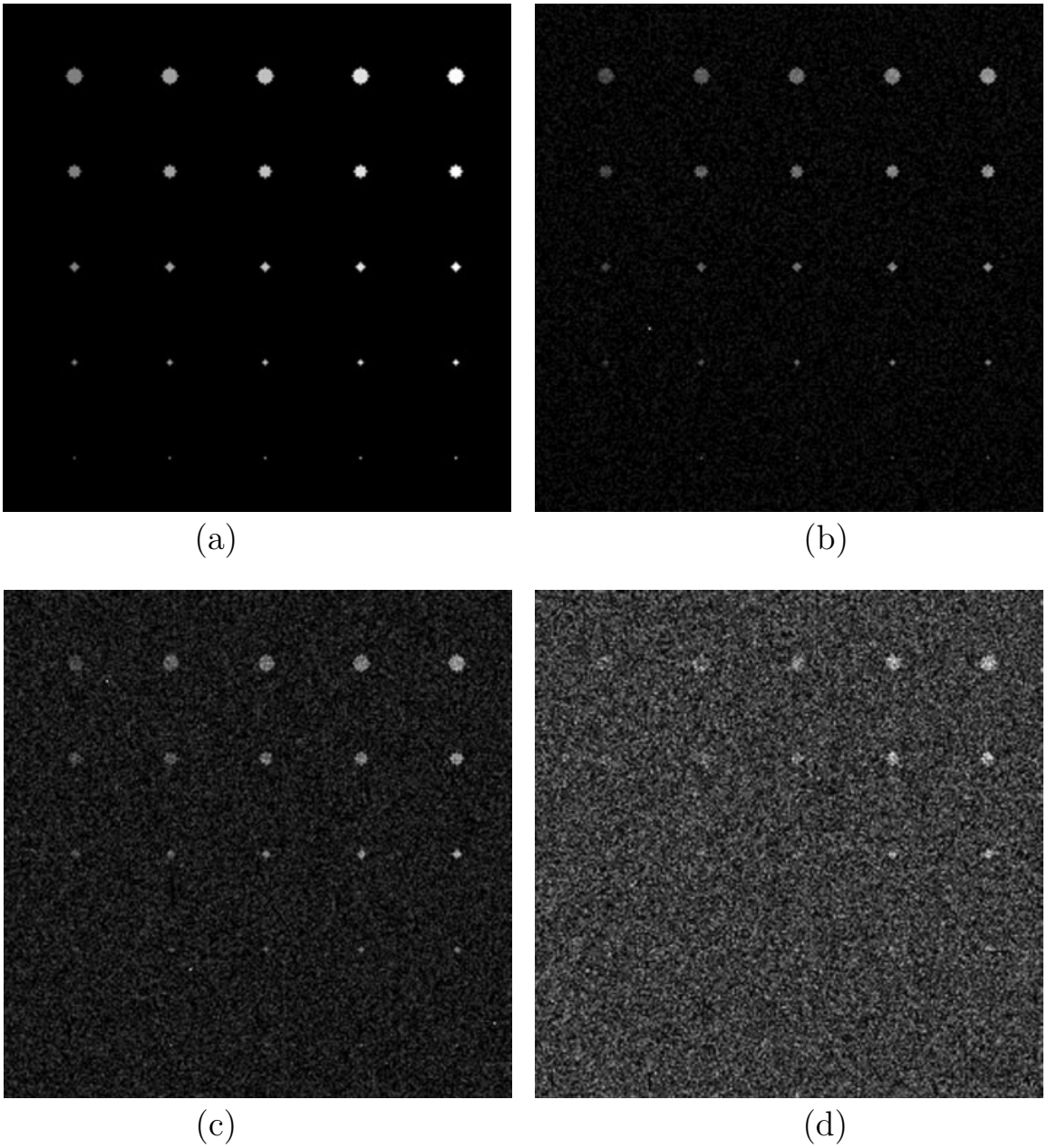

Fig. 15.5: Images designed to show how visibility of large and small objects changes as a function of CNR, and how their detection for a given CNR depends on the object size. For the cases shown, CNR is the same as SNR since each feature is being compared to the background noise. (a) Model of circles with no background noise (SNR = ∞); (b) SNR = 4; (c) SNR = 2; and (d) SNR = 1. (The SNR values quoted for these images are measured relative to the objects with lowest signal (column 1). As mentioned in the text, SNR doubles for the rightmost column in comparison with the leftmost column in each image.)

basic forms of contrast: spin-density weighted contrast, T_1-weighted contrast, and T_2- (or T_2^*-) weighted contrast.

A 90° gradient echo experiment is used as an example of how to obtain different forms of contrast. These results are identical to those that would be found for a 90° spin echo experiment under the assumption that $T_E \ll T_R$ and T_2 is replaced by T_2^*. Different expressions and relations must be derived for other imaging techniques.

15.4.1 Three Important Types of Contrast

Although each type of contrast is designed to enhance differences in one of the specified parameters (ρ_0, T_1, or T_2), the signal is a function of all three variables, and each must be kept in mind when determining overall image contrast. As an illustrative example, the contrast between tissues A and B for a 90° flip angle gradient echo experiment (see Fig. 15.6) is

$$C_{AB} = S_A(T_E) - S_B(T_E) = \rho_{0,A}(1 - e^{-T_R/T_{1,A}})e^{-T_E/T^*_{2,A}} - \rho_{0,B}(1 - e^{-T_R/T_{1,B}})e^{-T_E/T^*_{2,B}} \quad (15.43)$$

Note that the signal is assumed to be determined by the tissue signal solution from the Bloch equation at the echo time T_E. Remember, this time corresponds to the $k = 0$ sample in the read direction. C_{AB} can then be maximized with respect to either T_R or T_E.

15.4.2 Spin Density Weighting

In order to get contrast based primarily on ρ_0, the T_1 and T_2^* dependence of the gradient echo tissue signals must be minimized. When the argument of an exponential is small, an appropriate approximation to e^{-x} is $(1 - x)$ which is better written as $1 - \mathcal{O}(x)$. If the exponent is large and negative, e^{-x} can be approximated by zero. It is seen that in order to maintain adequate signal and get contrast based primarily upon spin density, appropriate choices of T_E and T_R would be

$$T_E \ll \quad T^*_{2_{A,B}} \Rightarrow e^{-T_E/T_2^*} \to 1 \quad (15.44)$$

$$T_R \gg \quad T_{1_{A,B}} \Rightarrow e^{-T_R/T_1} \to 0 \quad (15.45)$$

and expression (15.43) for the contrast between tissues becomes

$$\begin{aligned} C_{AB} &= (\rho_{0,A} - \rho_{0,B}) \\ &\quad -\rho_{0,A}\left(e^{-T_R/T_{1,A}} + \frac{T_E}{T^*_{2,A}}\right) + \rho_{0,B}\left(e^{-T_R/T_{1,B}} + \frac{T_E}{T^*_{2,B}}\right) \\ &\quad + \text{higher order and cross terms} \\ &\simeq \rho_{0,A} - \rho_{0,B} \end{aligned} \quad (15.46)$$

In this approximation, the contrast does not depend upon T_R or T_E, and need not be extremized relative to either T_R or T_E. This gives a general rule for spin density weighting: keep T_R much longer than the longest T_1 component; keep T_E much shorter than the shortest of $T^*_{2_{A,B}}$; the gradient echo image contrast is then primarily determined by spin density

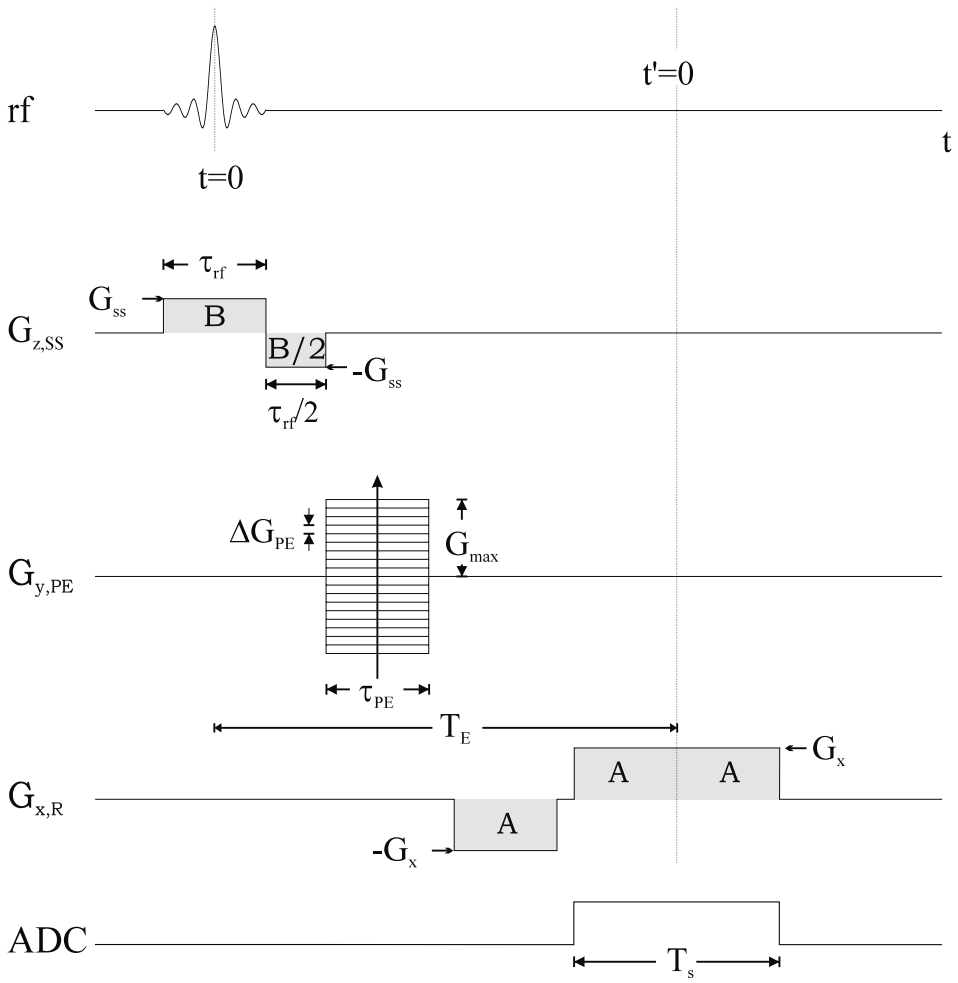

Fig. 15.6: A 2D gradient echo sequence diagram.

differences. Similar rules will be formed for T_1-weighting and T_2^*-weighting based on the practical limits imposed on T_E and T_R. These limits are summarized in Table 15.3. The actual error in this approximation of spin density weighting of the signal depends on the coefficients for T_E/T_2^* and T_R/T_1, the former vanishing only linearly in T_E/T_2^*. In practice, this means that most imaging experiments still have an error of a few percent even if T_E is as low as a few milliseconds since some typical T_2^* values are on the order of tens of milliseconds.

Problem 15.6

Estimating water content of one tissue relative to another from their contrast differences for a supposedly spin density weighted sequence may require including first-order effects of nonzero T_E and finite T_R. Consider a gradient echo experiment with $T_R = 5\,\text{sec}$, $T_E = 5\,\text{ms}$, and a $\pi/2$-pulse. Assume that ρ_0, T_1, and T_2^* for two adjacent tissues are 1.0, 2 sec, 40 ms and 0.8, 1 sec, 50 ms, respectively. The signal of the gradient echo dependence on T_E is found from

$$s = \rho_0(1 - e^{-T_R/T_1})e^{-T_E/T_2^*} \tag{15.47}$$

a) What are the effects of nonzero T_E and finite T_R on the contrast in this supposedly spin density weighted sequence?

b) The signal of the spin echo dependence on T_E is more complicated since

$$s = \rho_0(1 - 2e^{-(T_R-\tau)/T_1} + e^{-T_R/T_1})e^{-T_E/T_2} \tag{15.48}$$

Consider again T_R= 5 sec but T_E= 20 ms and a $\pi/2$-pulse, with T_2's of 40 ms and 50 ms respectively. How does the echo time affect contrast now?

Practically, the minimum T_E is limited by the available gradient strength. In fact, this limitation made the imaging of rigid solids impossible for many years because their T_2^* values are on the order of a few hundred microseconds to several milliseconds, and no hardware was available which could form an echo before the signal was gone. However, with modern hardware and modern imaging techniques, solids imaging is now viable. T_E is also limited by the highest acceptable readout bandwidth/voxel (or lowest possible T_s) for SNR and object visibility reasons. The maximum value of T_R, on the other hand, is constrained by imaging time and imaging efficiency reasons. Therefore, true spin density weighting using a 90° gradient echo sequence is practically achievable only for tissues with long enough T_2^*'s and short enough T_1's which allow T_E and T_R choices which satisfy the constraints imposed by the gradient strength limitation, the SNR and imaging time. Good spin density-weighted contrast is available for most purposes without requiring a zero T_E, or infinite T_R.

15.4.3 T_1-Weighting

Normal soft tissue T_1 values are quite different from one another. For this reason, T_1-weighted contrast offers a very powerful method for delineation of different tissues. To obtain spin density weighting, T_E and T_R were chosen to reduce the effect of T_1 and T_2. For T_1 and T_2 weighting, only the effects of T_2 and T_1 differences, respectively, can be minimized. The effects of spin density differences cannot be neglected.

For T_1 weighting, T_2^* effects have to be minimized. Using the gradient echo example as before, the choice of a very short T_E again reduces any T_2^* (or T_2) contrast, i.e., T_E is chosen such that

$$T_E \ll T^*_{2_{A,B}} \Rightarrow e^{-T_E/T_2^*} \to 1 \tag{15.49}$$

and the expression for the contrast is now

$$\begin{aligned} C_{AB} &= S_A(T_E) - S_B(T_E) \\ &\simeq \rho_{0,A}(1 - e^{-T_R/T_{1,A}}) - \rho_{0,B}(1 - e^{-T_R/T_{1,B}}) \quad T_E \ll T^*_{2_{A,B}} \\ &= (\rho_{0,A} - \rho_{0,B}) - (\rho_{0,A}e^{-T_R/T_{1,A}} - \rho_{0,B}e^{-T_R/T_{1,B}}) \end{aligned} \tag{15.50}$$

Since there is no transverse relaxation dependence in the above expression, this expression is equally valid for a spin echo sequence as well. It is typical that T_1 and T_2 correlate with

spin density, i.e., a tissue with higher spin density usually has longer T_1 and T_2 values, and tissues with lower spin density usually have shorter T_1 and T_2 values. As a result, while T_1 weighting depicts tissues with longer T_1 values with low signal and short-T_1 tissues with higher signal, the spin density contrast counteracts this effect. Hence, a unique choice of T_R which maximizes the T_1-weighted contrast should exist. To optimize the T_1-weighted contrast, (15.50) is extremized with respect to T_R. Differentiating C_{AB} with respect to T_R and setting it equal to zero leads to the relation

$$\frac{\rho_{0,A}e^{-T_R/T_{1,A}}}{T_{1,A}} = \frac{\rho_{0,B}e^{-T_R/T_{1,B}}}{T_{1,B}} \tag{15.51}$$

Solving for T_R from (15.51) gives the optimal T_R

$$T_{R_{opt}} = \frac{\ln\left(\frac{\rho_{0,B}}{T_{1,B}}\right) - \ln\left(\frac{\rho_{0,A}}{T_{1,A}}\right)}{\left(\frac{1}{T_{1,B}} - \frac{1}{T_{1,A}}\right)} \tag{15.52}$$

Some *a priori* knowledge of tissue properties is clearly very useful. When several tissues are present, it may be difficult to choose a single T_R which optimizes all contrast and two scans with two different T_R values would be required. In principle, T_1's of all tissues could then be found (see Ch. 22).

This optimal value of T_R can also be obtained graphically by plotting the expression for C_{AB} from (15.50) as a function of T_R. Consider one such plot shown in Fig. 15.7a. At long T_R values, all tissues will have relaxed completely, and only spin density contrast is obtained, i.e., the contrast curve approaches a constant value asymptotically. At low values of T_R such that $T_R \ll T_1$ (this defines the T_1-weighted contrast regime), where the signal is inversely proportional to T_1, the tissue with lower T_1 has a higher signal. In the case of gray matter and white matter, since white matter has the lower T_1, it has a higher signal at short T_R values. However, since white matter also has a smaller spin density than gray matter, once T_R becomes comparable to T_1, gray matter starts growing towards a higher value, crossing the white matter curve towards its higher spin density value. The crossover point represents a 'null point' between gray matter and white matter where there is no contrast. In between a T_R value of 0 where the contrast is zero and the null point, there must be a maximum, and this represents the T_R value which gives the optimal T_1-weighted gray matter/white matter contrast. Two other examples, GM/CSF (Fig. 15.7b) and GM/lesion[12] ($\rho_0 = 0.8$, $T_1 = 1.5\,\text{sec}$; Fig. 15.7c) are also shown for comparison. Again, the previous observations are obeyed in both cases, and the range of T_R choices for the spin density weighting or T_1 weighting regimes can be determined from these plots.

The presence of a null point in the contrast curves was already noted. Its determination for the particular case of GM/WM contrast is the subject of Prob. 15.7.

[12] A 'lesion' is used to indicate abnormal tissue which contains T_1 and T_2 values larger than those of normal gray matter.

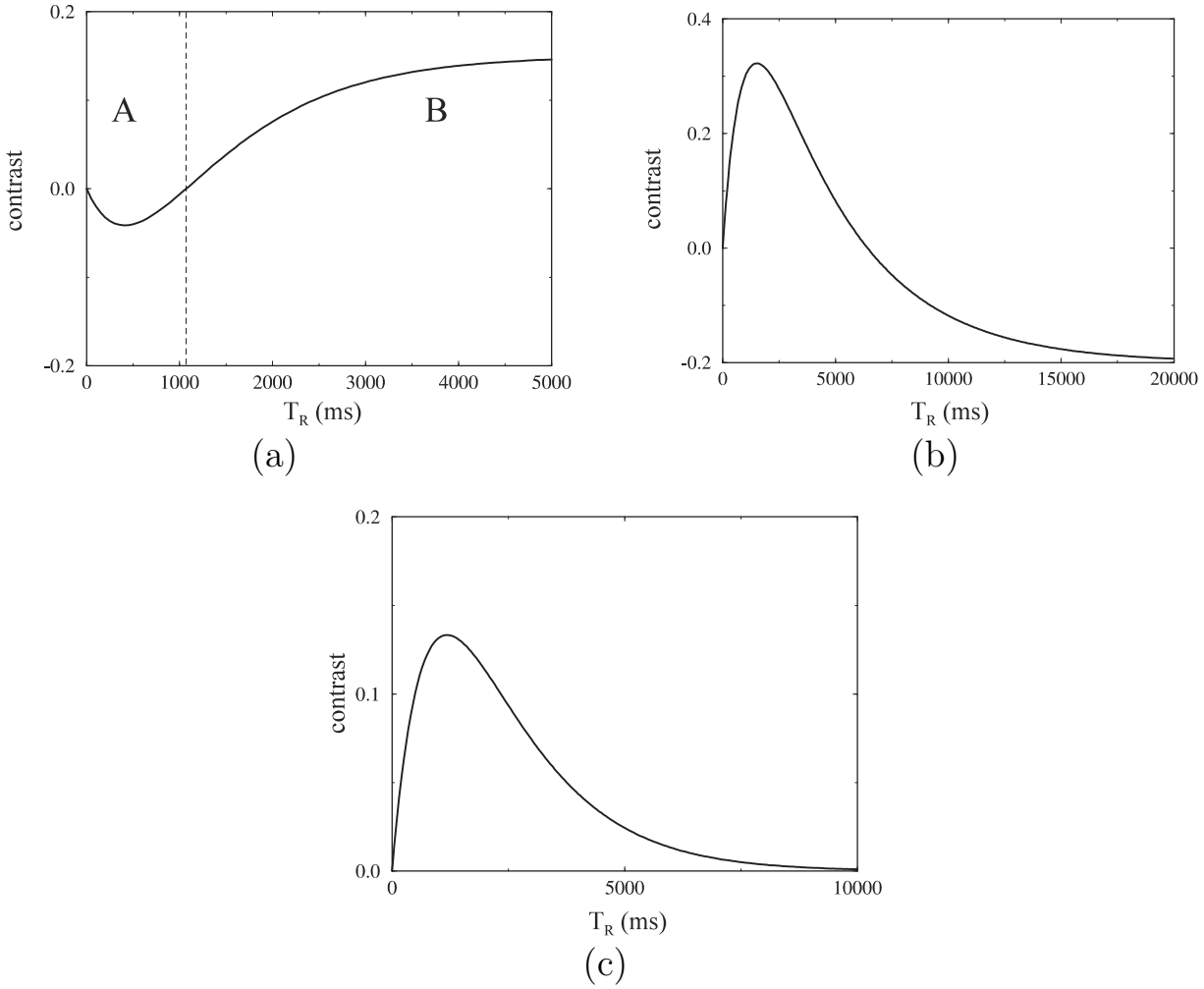

Fig. 15.7: C_{AB} as a function of T_R for (a) GM/WM (b) GM/CSF (c) GM/lesion in the case of a T_1-weighted 2D or 3D imaging experiment assuming ideal rf pulses. As demarcated in (a), two regions can be identified for each plot: one where the contrast is T_1 weighted (region A in (a) for example), and another where the contrast is spin density-weighted (region B in (a) for example). The figure shows that a unique T_R value which optimizes either contrast can be identified for each tissue pair of interest (which varies according to the intended application). The tissue parameters ρ_0 and T_1 used to simulate these figures came from Table 4.1 in Ch. 4. The lesion parameters were chosen to be $\rho_0 = 0.8$ and $T_1 = 1.5\,\text{sec}$.

Problem 15.7

a) Show that for a 90° flip angle, short-T_E gradient echo sequence, there is a choice of T_R where gray matter (gray matter spin density relative to water = 0.8; T_1 = 950 ms at 1.5 T) and white matter (white matter spin density relative to water = 0.65; T_1 = 600 ms at 1.5 T) are iso-intense (i.e., they have the same signal). This represents a 'crossover point' on the contrast curve. What T_R does this crossover occur at?

b) Explain why there is such a crossover point (a plot of the two signals as a function of T_R would be helpful in making your argument).

c) From (15.52), find the T_R which optimizes the gray matter/white matter contrast.

The reader will find that these values are not perfect in real studies since the rf slice profile is not a boxcar function and all of the spins in the slice are not tipped by $\pi/2$. When this occurs, the tissues behave as if they have shorter than expected T_1.

Optimal T_R for Tissues with Similar Spin Densities and Fractionally Different T_1

The optimal value for T_R obtained in (15.52) represents the most general case of two tissues A and B which have different spin densities. In the early stages of the formation of certain diseased states, it is not uncommon to find the diseased tissue with a spin density which is very comparable to its normal neighbor, i.e.,

$$\rho_{0,A} \simeq \rho_{0,B} \equiv \rho_0 \tag{15.53}$$

and a T_1 which is fractionally different. That is,

$$T_{1,B} = T_{1,A}(1+\delta) \quad \text{with} \quad \delta \to 0 \tag{15.54}$$

The expression for the contrast is

$$\begin{aligned} C_{AB} &= \rho_0 e^{-T_R/T_{1,A}} - e^{-T_R/((1+\delta)T_{1,A})} \\ &\simeq \rho_0 e^{-T_R/T_{1,A}} \left(e^{\delta T_R/T_{1,A}} - 1\right) \quad \text{since} \quad e^{-T_R/(1+\delta)T_{1,A}} \simeq e^{-(1-\delta)T_R/T_{1,A}} \\ &\simeq \rho_0 e^{-T_R/T_{1,A}} \left(\frac{T_R}{T_{1,A}}\right) \cdot \delta \end{aligned} \tag{15.55}$$

which is again a function of T_R. Maximizing with respect to T_R then yields

$$T_{R_{opt}} = T_{1,A} \tag{15.56}$$

i.e., for two tissues with comparable spin density and slightly different T_1 values, the optimal T_R to choose is the T_1 value of the shorter T_1 tissue.

A similar approach can be taken for the arbitrary flip angle steady state incoherent method discussed in Sec. 18.1.5.

Problem 15.8

Derive an expression similar to (15.56) for a general value of δ. How does this value of $T_{R_{opt}}$ normalized to $T_{1,A}$ compare with the choice of a T_R of an average value of $T_{1,A}$ and $T_{1,B}$ normalized to $T_{1,A}$? What is the range of δ values up to which the average value serves as a reasonable approximation to the optimal T_R? The fact that the contrast is optimized by a T_R value comparable to the average of the T_1 values of the two tissues is used as a general rule of thumb for choosing T_R for tissues with comparable spin density values.

15.4.4 T_2^*-Weighting

The third basic contrast generating mechanism is based on differences in the transverse decay characteristics. Most disease states are characterized by an elevated T_2. Since the T_2 values are only on the order of tens of milliseconds whereas T_1 values are typically on the order of a second, a small increase in T_2 corresponds to a larger percentage increase than the same increase in T_1. As a result, T_2 is found to be a sensitive indicator of disease. T_2 weighting can be obtained by using spin echo sequences. T_2^* weighting also plays a useful role when local magnetic field susceptibility differences between tissues are present. If field changes occur sufficiently rapidly across a voxel, additional signal loss will occur when gradient echo sequences are used. For this reason, T_2^*-weighted images are used to study brain activity in brain functional imaging studies (as discussed in Ch. 25).

To avoid contributions from T_1 confounding the contrast, T_R is chosen such that[13]

$$T_R \gg \quad T_{1_{A,B}} \Rightarrow e^{-T_R/T_1} \rightarrow 0 \tag{15.57}$$

in which case the gradient echo contrast is given by

$$C_{AB} = \rho_{0,A} e^{-T_E/T_{2,A}^*} - \rho_{0,B} e^{-T_E/T_{2,B}^*} \tag{15.58}$$

Figure 15.8b shows a plot of T_E versus contrast for (15.58) using gray matter ($\rho_0 = 0.8$ and $T_2 = 0.1\,\text{sec}$) and CSF ($\rho_0 = 1.0$ and $T_2 = 2\,\text{sec}$) as tissues A and B. Since GM has a T_2 value which is much shorter than that of CSF, the optimal T_E value is expected to be long compared to the T_2 value of gray matter and short compared to the T_2 value of CSF. On the other hand, when gray and white matter signals are considered as functions of T_E at long T_R values (Fig. 15.8a), WM ($\rho_0 = 0.65$ and $T_2 = 0.08\,\text{sec}$) always has a signal that is lower than that of GM. So, the optimal GM/WM contrast is produced by a very short T_E, in the spin density-weighted regime. A similar contrast curve can be generated for any two tissues

[13]It is also possible to obtain spin density or T_2^*-weighting with shorter T_R but then the rf pulse angle must be reduced to a value much less than $\pi/2$. A discussion of this class of experiments is reserved for the fast imaging discussion in Ch. 18.

of interest, whose relative spin density and T_2 values are known. For example, the case of GM/lesion contrast is considered in Fig. 15.8c. The lesion is assumed to have a ρ_0 of 0.8 and a T_2 of 350 ms. Since the contrast expression (15.58) contains only T_E dependence, optimal contrast is obtained by extremizing C_{AB} relative to T_E. The T_E at which the contrast is optimized is

$$T_{E_{opt}} = \frac{\ln\left(\frac{\rho_{0,B}}{T^*_{2,B}}\right) - \ln\left(\frac{\rho_{0,A}}{T^*_{2,A}}\right)}{\left(\frac{1}{T^*_{2,B}} - \frac{1}{T^*_{2,A}}\right)} \tag{15.59}$$

As previously discussed, a similar expression is obtained for a spin echo experiment in terms of T_E with T_2^* replaced by T_2. Expressions for the optimal T_E in the special case of only a fractional difference in T_2 also gives results identical in form to the T_R choice for optimal

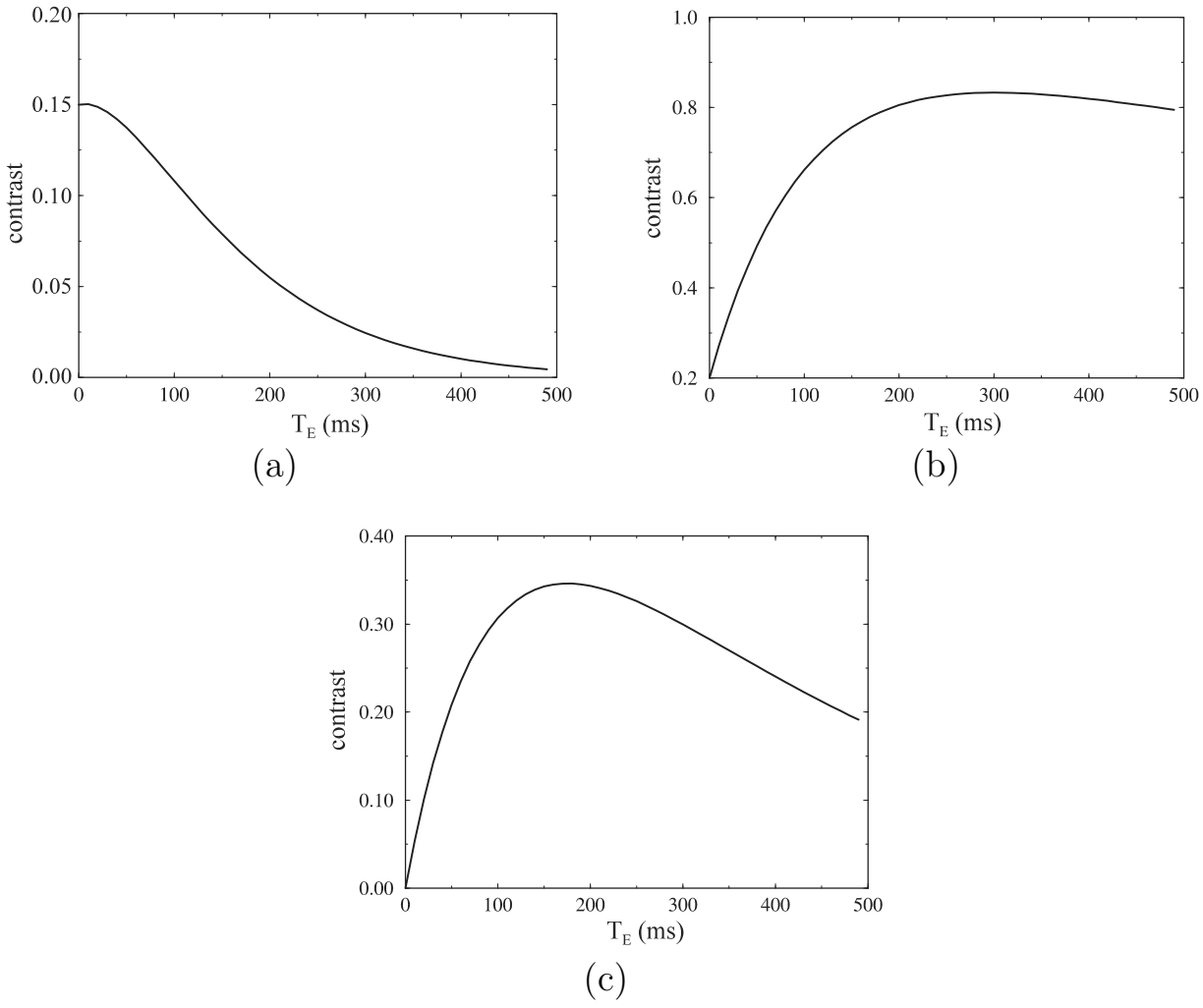

Fig. 15.8: C_{AB} as a function of T_E for (a) GM/WM (b) CSF/GM and (c) lesion/GM for a T_2-weighted scan. C_{AB} is given in units relative to a maximal value of unity. An optimal T_E value can also be obtained for each pair of tissues from such plots.

T_1-weighted contrast: that is, a T_E approximately equal to $T^*_{2,A}$ should be chosen.

Problem 15.9

---

a) Suppose that the relative spin density (ρ_0), T_1, and T_2 values of a certain tissue (gray matter, say) are 0.8, 1 s, and 100 ms, respectively. When disease sets in, suppose the local water content increases from 0 to 10% in each voxel. This two-compartment model implies that the fractional volume content of water in a voxel increases from 0 to 0.1 and that of the tissue decreases from 1.0 to 0.9. (This can happen when edema forms.) If the T_1 and T_2 of water are 4 s and 2 s, respectively, and the R_1 and R_2 values of healthy tissue and water average according to volume fraction of occupation of the voxel, what are the percentage increases in the effective T_1 and T_2 values in the diseased tissue?

b) Hence, which of the two mechanisms, T_1- or T_2-weighting, is more sensitive to small changes in local water content (compare the percentage change from values in normal tissues between T_1 and T_2)?

c) Find the optimal T_E for distinguishing this 'diseased tissue' from its normal neighbor, neglecting the change in spin density. Hence, show that the optimal T_E in the case of two tissues with comparable spin densities but different T_2 values such that $T_{2_B} = T_{2_A}(1 + \delta)$ is comparable to the average of the two T_2 values.

The conclusion from Prob. 15.9 is that T_2-weighting might be the intrinsic contrast mechanism of choice for distinguishing diseased states from normal tissue. In fact, it therefore comes as no surprise that T_2-weighted spin echo sequences are used for a variety of clinical applications.

15.4.5 Summary of Contrast Results

The general appearance of spin density, T_1- and T_2-weighted images of the brain is depicted in the images shown in Fig. 15.9. An optimal and yet practicable set of imaging parameters was used to obtain these images. Clearly, the T_1-weighted imaging method seems to be the most efficient in achieving the contrast required. An intermediate T_R value of about 600 ms gives optimal GM/WM contrast and shows good differentiation between these two structures and CSF and fat. Fat, with the lowest T_1 value amongst these four tissues, is shown as the brightest structure. On the other hand, CSF is shown with almost no noticeable signal because of its long T_1. White matter is the structure which is shown as the bright structure in the brain, while gray matter is shown with a lower gray level, all consistent with T_1 weighting. On the other hand, when it comes to spin density or T_2 weighting, it is impractical to design the sequence with a T_R which is on the order of a few T_1's of CSF. Therefore, it is typical to choose a T_R of about twice the T_1 of gray matter. At this T_R, CSF is almost iso-intense with white matter, and gray matter is found to have the highest signal. As described here, the

spin density and T_2-weighted images shown in Figs. 15.9a and 15.9b were obtained using a T_R of 2.5 sec. On the T_2-weighted image, typically obtained using a longer T_E at the same T_R as the spin density-weighted image, CSF has the highest signal while white matter has the lowest signal. A set of general rules for choosing T_E and T_R for a $\pi/2$ gradient echo (or spin echo) experiment are outlined in Table 15.3.

Type of contrast	T_R	T_E
spin density	as long as possible	as short as possible
T_1-weighted	on the order of the T_1 values	as short as possible
T_2-weighted	as long as possible	on the order of the T_2 values

Table 15.3: General set of rules for generating tissue contrast.

Problem 15.10

Tissues A and B are found to have the following properties when imaged at a certain field strength

Quantity	A	B
T_1	600 ms	300 ms
intrinsic T_2^* ($\Delta B_0 = 0$)	80 ms	60 ms
normalized ρ_0	1.0	0.8

Assume that $\rho_{0,A}/\sigma_0$ is 40:1 and, in order for two tissues to be reliably differentiated, that the CNR must be greater than or equal to 4. Consider the gradient echo example presented earlier in this section.

a) If T_E is kept short (say $T_E = 20$ ms) to minimize T_2^* contrast, what is the minimum value of T_R that may be used to obtain a T_1-weighted image with adequate CNR such that A and B are reliably differentiated?

b) If T_R is 2000 ms, find the minimum and maximum values of T_E that could be used to obtain a T_2-weighted image with adequate CNR.

15.4.6 A Special Case: T_1-Weighting and Tissue Nulling with Inversion Recovery

Another commonly used mechanism for generating T_1 contrast is to use an inversion recovery (IR) sequence. Image contrast with the inversion recovery sequence can be adjusted with both T_R and T_I. There is interest in finding out the most time-efficient way to obtain T_1 weighting at some value (not necessarily the optimal value) of T_R or T_I. This is obtained by

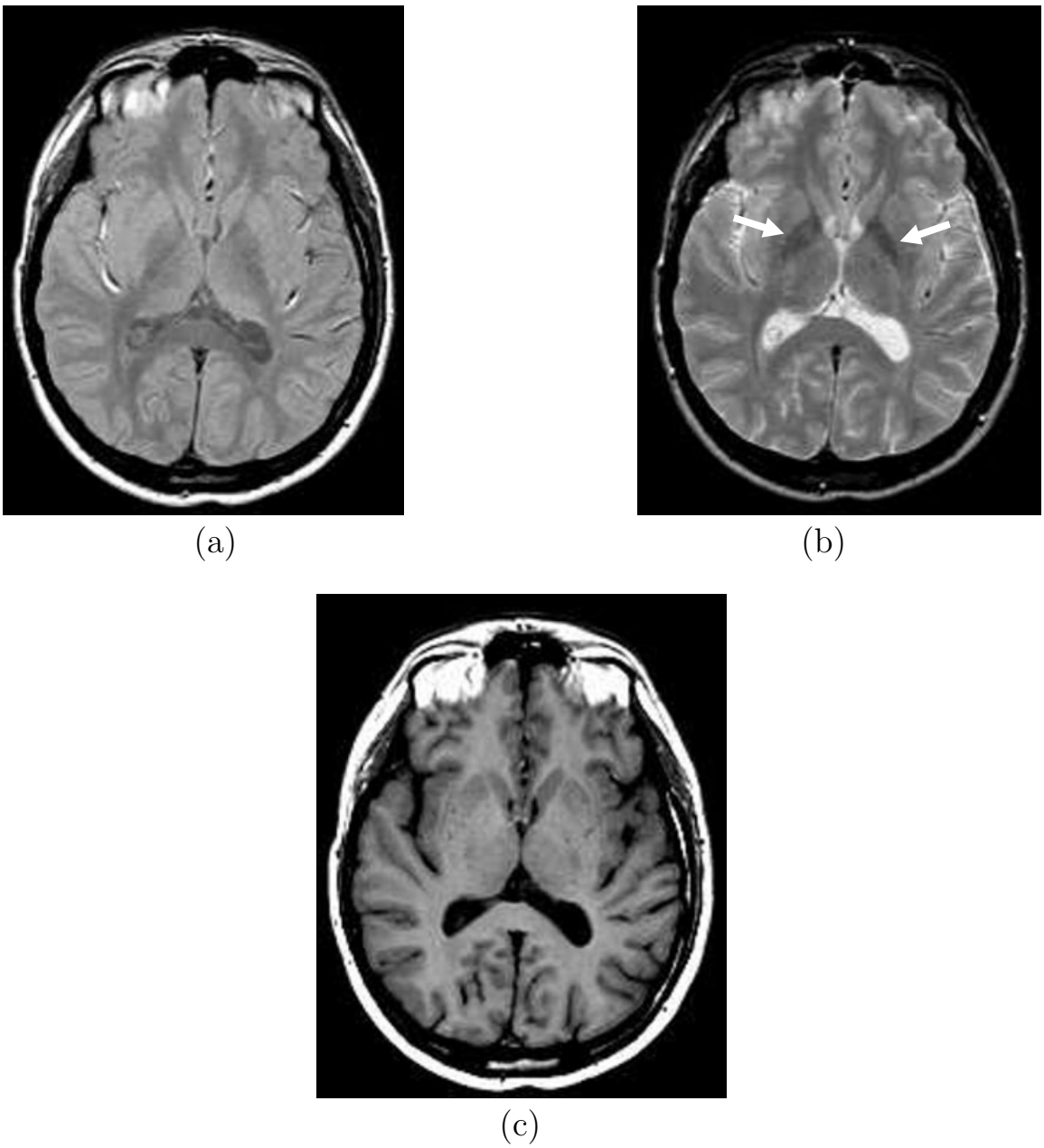

Fig. 15.9: Different forms of contrast generated by varying the imaging parameters with a spin echo sequence. (a) Spin density-weighted image. (b) T_2-weighted image. (c) T_1-weighted image. Although (a) is supposed to indicate spin density, it fails to do so for CSF since T_1 of CSF is too long (4.5 sec) relative to the T_R (2.5 sec). Gray/white matter contrast is good. In (b), the globus pallidus (arrow) appears quite dark (since the iron in it causes a diffusion weighted signal loss; see Ch. 21). As expected, CSF is bright because of its long T_2 (2 sec). Lastly, in (c), gray/white matter contrast is reversed and CSF is heavily suppressed. The dark CSF regions seem to visually enhance the overall contrast in the image.

looking at the differential change in signal relative to a differential increase in T_R or T_I. For the gradient echo sequence,

$$\frac{\partial C_{AB}}{\partial T_R} = \rho_{0,A}\frac{T_R}{T_{1,A}}e^{-T_R/T_{1,A}} - \rho_{0,B}\frac{T_R}{T_{1,B}}e^{-T_R/T_{1,B}} \tag{15.60}$$

whereas, for the inversion-recovery sequence (whose signal expression is given by (8.46))

$$\frac{\partial C_{AB}}{\partial T_I} = 2\left(\rho_{0,A}\frac{T_I}{T_{1,A}}e^{-T_I/T_{1,A}} - \rho_{0,B}\frac{T_I}{T_{1,B}}e^{-T_I/T_{1,B}}\right) \quad \text{for } T_R \gg T_1 \tag{15.61}$$

i.e., for the same increase in T_R or T_I, the inversion-recovery signal has twice the signal change as the spin echo signal change. If two tissues with only fractional T_1 differences are considered, this directly correlates to a doubling of the contrast in the inversion-recovery sequence. This was the reason for the early popularity of the inversion-recovery sequence for obtaining T_1 weighting.

The inversion process offers the ability to null a specific tissue by an appropriate choice of T_I. Some examples of this feature unique to the inversion recovery sequence are shown in Fig. 15.10. Here, four different choices of T_I can be used to null fat, white matter, gray matter, and cerebrospinal fluid, respectively. The first three are used in T_1-weighted IR imaging methods and the fourth in a T_2-weighted sequence to better differentiate small lesions otherwise obscured by CSF. The first is useful to image near the orbits where fat can obscure the optic nerve, for example. The third shows a more conventional T_1-weighted image. The fourth nulls CSF and any other water-like components but leaves good signal from pathological states with only slightly elevated water content relative to normal tissue.

Problem 15.11

Consider the implementation of an inversion-recovery sequence with T_I chosen to null the signal (implies $T_{I,null} = T_1 \ln 2$ in the limit that $T_R \gg T_1$) for either fat or water at 1.5 T. Find $T_{I,null}$ for water and fat whose T_1 values are $T_{1,w} = 4\,\text{s}$ and $T_{1,f} = 250\,\text{ms}$, respectively.

15.5 Contrast Enhancement with T_1-Shortening Agents

In fast imaging, where T_R is much less than T_1, the signal for a 90° flip angle is proportional to T_R/T_1 and, in this regime, tissues with shorter T_1 have a higher signal than tissues with longer T_1 and the contrast is predominantly T_1-weighted.

Certain external agents can be introduced into specific targeted tissues where these agents act to reduce the T_1 of that tissue. Figure 15.11 demonstrates the T_1-shortening effect of one of these agents. Suppose that the targeted tissue (in the case shown in Fig. 15.11, the targeted tissue is blood) has similar NMR properties as its neighboring tissue, causing an inability to differentiate the two using any of the three contrast mechanisms discussed in Sec. 15.4 but contains a different signal response to the contrast agent. By delivering the

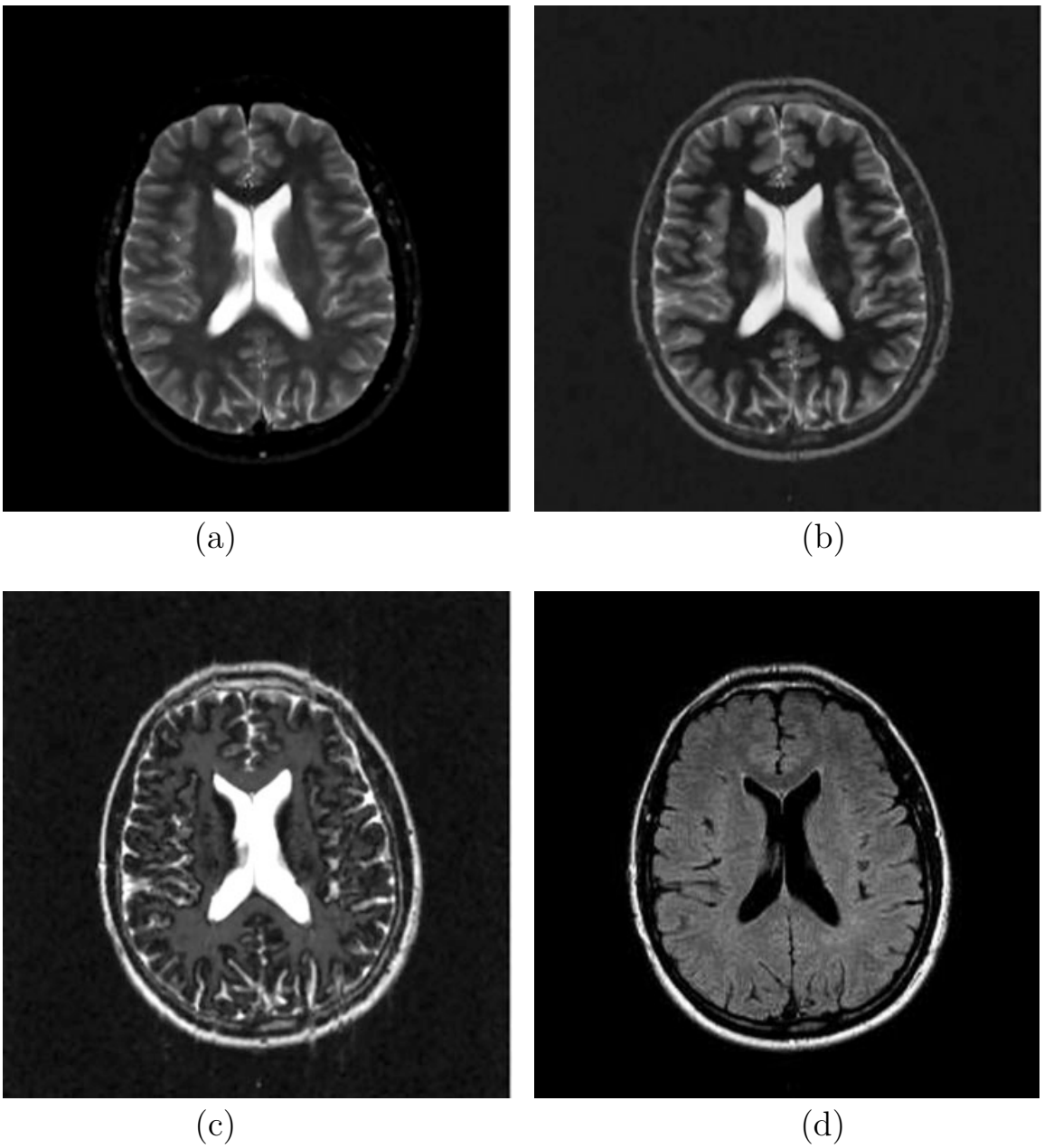

Fig. 15.10: Different tissues nulled with an inversion recovery sequence. (a) A short T_I is chosen to null fat. (b) An intermediate T_I is chosen to null WM. (c) A higher T_I nulls GM. (d) A very long T_I nulls CSF, which is typically used in a T_2-weighted sequence to null the otherwise very high signal producing CSF.

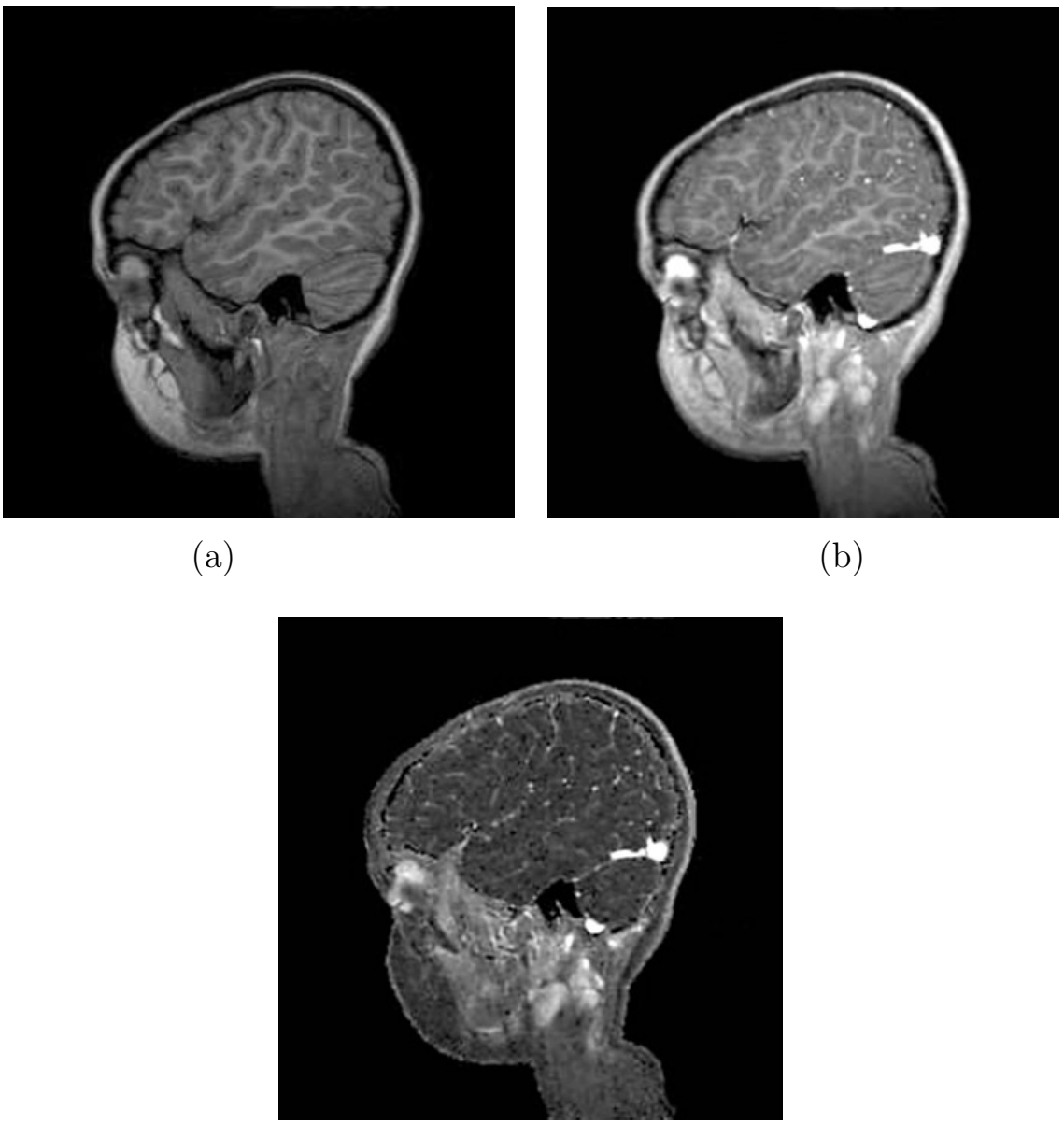

Fig. 15.11: T_1 reduction effects of a contrast agent. (a) A single slice from a 3D T_1-weighted data set before contrast agent was injected. (b) Image of the same slice after an intravenous injection of a T_1-shortening contrast agent. Since the T_1 of blood is shortened, the blood vessels light up, and are seen as bright spots in the image. Also, there is a loss of contrast between WM/GM because of the larger blood volume content of GM (hence, its signal increases more than that of WM, reducing contrast). (c) Subtraction of the first image from the second image depicts this signal increase predominantly in the blood vessels, but also from the blood-containing tissue itself. Only those voxels with a positive subtraction are shown; voxels with a negative subtraction are set to zero, leading to the isolated black dots in this image.

T_1-shortening agent to the tissue of interest, the targeted signal is increased while the signal from the background remains the same when a T_1-weighted sequence is used. This increases the contrast between the two tissues and, for this reason, such agents are commonly referred to as 'contrast agents.'

In general, the increase in relaxation rate after T_1 shortening is found to be directly proportional to the concentration C of the contrast agent delivered to the tissue. If $T_{1,0}$ is the intrinsic T_1 of the tissue and $T_1(C)$ is its shortened value, it is found that

$$\begin{aligned} R_1(C) \equiv \frac{1}{T_1(C)} &= \frac{1}{T_{1,0}} + \alpha_1 C \\ &\equiv R_{1,0} + \alpha_1 C \end{aligned} \tag{15.62}$$

where the constant of proportionality α_1 is called the longitudinal relaxivity (T_1 relaxivity) with units of $(\text{mmol/l})^{-1}\text{sec}^{-1}$,[14] a property specific to the composition of the contrast agent. Figure 15.12a demonstrates the effect of a contrast agent *in vivo* on the T_1 of blood for which $T_{1,0} \simeq 1200\,\text{ms}$ at 1.5 T.

Problem 15.12

If a contrast agent at a dose of 0.1 mmol/kg is given to a 50 kg person with 5 liters of blood in his/her body, what is the expected T_1 of the blood when the contrast agent is well-mixed in the blood? Assume the T_1-relaxivity of the contrast agent is 5/mM/sec and T_1 of blood is 1200 ms. In practice, some of the agent is taken up by other organs in the body and this 'extravasation' can lead to the effective blood volume (or effective distributed volume of the contrast agent) being 10 liters for purposes of this calculation. How does this affect the above estimate for T_1?

In addition to shortening the T_1, these contrast agents also tend to shorten the T_2 of the tissue in a similar fashion to the T_1 shortening, i.e.,

$$\begin{aligned} R_2(C) \equiv \frac{1}{T_2(C)} &= \frac{1}{T_{2,0}} + \alpha_2 C \\ &= R_{2,0} + \alpha_2 C \end{aligned} \tag{15.63}$$

where α_2 is the transverse relaxivity of the contrast agent. Figure 15.12b shows the effect of contrast agent dosage on the T_2 of blood (which has an intrinsic T_2 ranging from 100 ms for venous blood to 200 ms for arterial blood). This concomitant decrease in T_2 tends to partly counterbalance the effects of shortened T_1. For many T_1-shortening contrast agents, the transverse and longitudinal relaxation rates are comparable in magnitude ($\alpha_1 \simeq \alpha_2$). Since $R_{2,0} > R_{1,0}$, a given increase in the concentration leads to a larger magnitude change in T_1 and, hence, in the signal due to this shortened T_1 effect than the effect caused by the T_2 reduction. It is only when $\alpha_2 C$ becomes comparable to $R_{2,0}$ that the signal loss due to the T_2 shortening becomes significant, and starts to overwhelm the enhanced T_1-weighted

[14] Recall that 1 mmol/l is also written as 1 mM (millimolar).

contrast. In fact, this crossover point between signal loss due to T_2 shortening and signal increase due to T_1 shortening defines an optimal contrast agent dosage.

A major clinical application of T_1 shortening contrast agents at present is intended for the improved detection of small lesions. Typically, these lesions have a fractionally increased water content leading to best depiction of these lesions in a T_2-weighted image before contrast agent is injected. Despite being the most sensitive contrast mechanism, it is not possible for the T_2-weighted image to depict very small lesions which are averaged with neighboring tissue of comparable NMR tissue properties. The use of an intravenous injection of a T_1

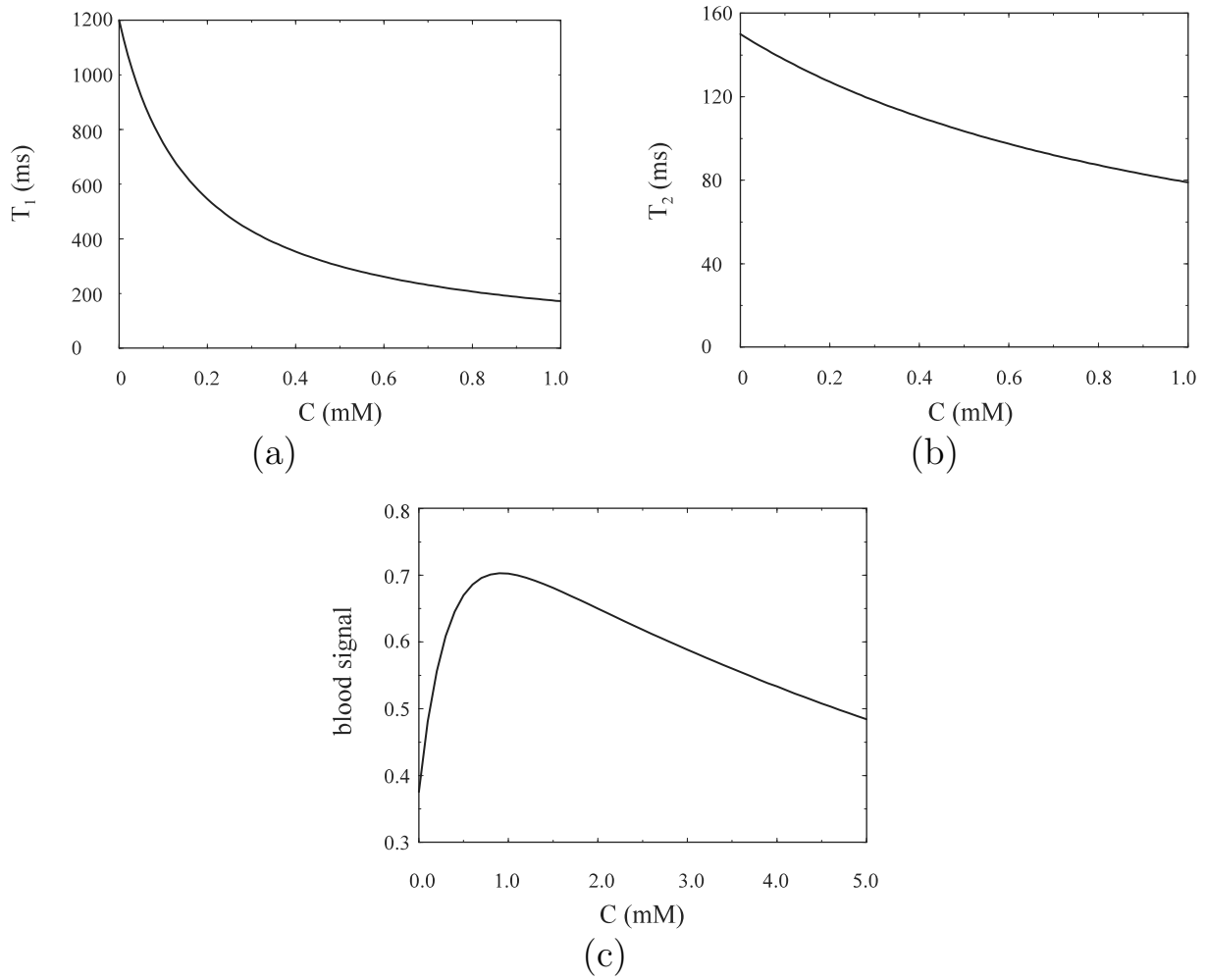

Fig. 15.12: T_1 and T_2 are plotted in (a) and (b), respectively, as functions of contrast agent concentration delivered to the tissue of interest. The contrast agent is supposed to have longitudinal and transverse relaxivities of 5 /mM/sec and 6 /mM/sec, respectively. Notice that the relative change in T_1 for a given concentration is much larger than that for T_2. (c) Blood signal in relative units as a function of contrast agent concentration plotted for a spin echo acquisition with 600 ms T_R and 20 ms T_E. (T_1 and T_2 of blood were taken to be 1200 ms and 150 ms, respectively.) Note that, as the concentration increases, the T_2 reduction effect takes over and causes a reduction of blood signal. In essence, an optimal concentration which maximizes the signal exists.

shortening agent is indicated for such patients. Most lesions are found to have a rich blood supply. Therefore, the lesions have contrast agent delivered locally, leading to lesion signal enhancement and improved lesion detection.

15.6 Partial Volume Effects, CNR, and Resolution

In the earlier discussion on object visibility, it was seen that $\mathcal{V}$ is invariant as a function of voxel size for multi-voxel objects under the assumption that the voxel signal came from a homogeneous chunk of tissue within the voxel. What then is the advantage of using a smaller voxel size if reducing the voxel size serves only to worsen the SNR while only maintaining object visibility? In this section, resolution effects on object visibility are discussed in detail, leading to a theoretical understanding of the effects of spatial resolution on the diagnostic value of an image.

If tissue A is smaller than a voxel, it shares the voxel with the background tissue, and tissue A is said to be 'partial volumed.' Such a partial volume model is shown in Fig. 15.13. If the point spread effects of the image reconstruction are neglected, a simple model for the combined signal from the voxel is the summed fractional signals of tissues A and B. Let S_A and S_B represent the signal for tissues A and B, respectively, when they occupy an entire voxel of size Δx (i.e., S_A is the signal from tissue A if α equals 1 in Fig. 15.13a). In the

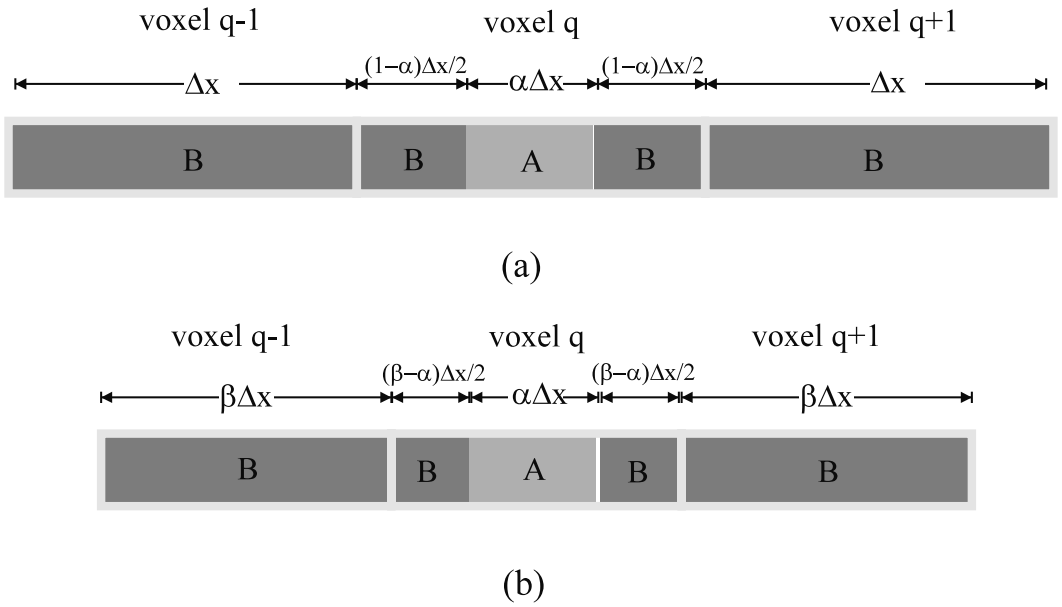

Fig. 15.13: Model of a 1D voxel q which is occupied by two different materials or tissues. Voxels $(q-1)$ and $(q+1)$ contain only background tissue with signal magnitude S_B in (a) where the voxel size is Δx, while the central voxel q contains a combination of tissues A and B, with tissue A of size $\alpha\Delta x$ ($\alpha < 1$) occupying a fraction α of the voxel. In (b), the voxel size is reduced to $\beta\Delta x$ ($\beta < 1$) and tissue A now occupies the fraction α/β of the central voxel while the signal from voxels $(q-1)$ and $(q+1)$ are also reduced to βS_B.

general case, if α is the fraction of voxel q occupied by tissue A, the signal for voxel q when $\beta = 1$ (Fig. 15.13a) is the sum of the voxel signal contributions $\hat{\rho}_{A,q}$ and $\hat{\rho}_{B,q}$ from A and B, respectively, i.e.,

$$\hat{\rho}_{voxel,q} = \hat{\rho}_{A,q} + \hat{\rho}_{B,q} \tag{15.64}$$

Now

$$\hat{\rho}_{A,q} \equiv \alpha S_A \quad \text{and} \tag{15.65}$$
$$\hat{\rho}_{B,q} \equiv (1-\alpha) S_B \tag{15.66}$$

and hence from (15.64)

$$\hat{\rho}_{voxel,q} = \alpha S_A + (1-\alpha) S_B \tag{15.67}$$

The image contrast is then

$$C_{q,q+1} = \underbrace{\hat{\rho}_{voxel,q}}_{\text{voxel with A and B}} - \underbrace{\hat{\rho}_{voxel,q+1}}_{\text{homogeneous voxel with B}} = \alpha(S_A - S_B) \tag{15.68}$$

The conclusion is that if a certain tissue is partial volumed, its contrast is reduced according to the fraction of the voxel it is occupying.

In the case where the voxel size is reduced, i.e., $\beta < 1$, tissue A occupies the fraction $\frac{\alpha}{\beta}$ of the entire voxel volume and B occupies the remaining $1 - \frac{\alpha}{\beta}$ fraction of the voxel. Also, the signal from voxels $q-1$ and $q+1$ is now βS_B. In a similar fashion, the signal from A, when it occupies a complete voxel of size $\beta \Delta x$, is βS_A, leading to

$$\hat{\rho}_{q,A} \to \frac{\alpha}{\beta}(\beta S_A) \tag{15.69}$$

and

$$\hat{\rho}_{q,B} \to \frac{(\beta - \alpha)}{\beta}(\beta S_B) = (\beta - \alpha) S_B \tag{15.70}$$

Hence the contrast is

$$C_{q,q+1}|_{\beta<1} = \hat{\rho}_{voxel,q} - \hat{\rho}_{voxel,q\pm1} = (\alpha S_A + (\beta - \alpha) S_B) - \beta S_B = \alpha(S_A - S_B) \tag{15.71}$$

i.e., the contrast does not change.

Two cases can be considered for increasing the spatial resolution (say, making $\beta \to \beta/2$): case 1, doubling T_s or the number of phase encoding steps so that the SNR reduces by only $\sqrt{2}$ and case 2, halving the FOV keeping N fixed, leading to a loss of 2 in SNR. As the voxel size is decreased by a factor of 2, the CNR (and visibility) increases by $\sqrt{2}$ in case 1 and stays the same in case 2. If the SNR is good enough, this result indicates it is possible that a small partial volumed object will become visible as Δx is reduced.

In summary, the utility of high resolution lies in its ability to make partial volumed objects which are smaller than the voxel size visible, even though the SNR decreases as Δx is reduced. Although at first sight it seems like tissue A has been conveniently chosen to be at the center of the voxel in (a) for this improved visibility result, even in the more general case of an arbitrarily positioned A, it can always be moved into the center of the

voxel by using the Fourier transform shift theorem (see Ch. 11 for details) for which case this improved visibility result holds.

Problem 15.13

Consider an object of size $\Delta x/4$ (say a small blood vessel) and centered in a 1D voxel of size Δx as shown in Fig. 15.14a. Suppose $(S_A - S_B)/\sigma_0$ is 2.0 when the voxel size is Δx. Now suppose the voxel size is halved (case 1) to $\Delta x/2$ (see Fig. 15.14b) and then halved again (case 2) to $\Delta x/4$ (see Fig. 15.14c).

a) If S_q/σ is 8.0 when the voxel size is Δx, what is the SNR at the two smaller voxel sizes shown in Figs. 15.14b and 15.14c? Assume that SNR_q is reduced by $\sqrt{2}$ each time the resolution is halved. The common misconception is that because the SNR is reduced, the diagnostic value of the image is lost. Evidently, object visibility, rather than SNR, is the more appropriate index of clinical utility.

b) What happens to $\mathcal{V}$ at the two smaller voxel sizes in (i) case 1, and (ii) case 2? Is the object visible at any of the three voxel sizes (i) in case 1, and (ii) case 2? Assume that the visibility threshold is 3. The important point is that if there is an object of interest which is invisible at a given voxel size because of partial volume effects, it may be possible to make it visible by reducing the voxel size. Other additional options include using a contrast agent to increase signal or averaging over multiple acquisitions to reduce the noise.

15.7 SNR in Magnitude and Phase Images

Phase offers some fascinating ways to enhance information about certain features in MR images. When the field is perfect and no motion is present, the expected phase is zero. White noise will also have a magnitude and phase. We consider here the contribution of noise to the magnitude and phase images ($|\hat{\rho}|$ and $\hat{\phi}$) in the case where the SNR is much greater than unity.

15.7.1 Magnitude Image SNR

The complex signal can be written as

$$\hat{\rho} = R + iI \tag{15.72}$$

or as

$$\hat{\rho} = \rho_m e^{i\phi} \tag{15.73}$$

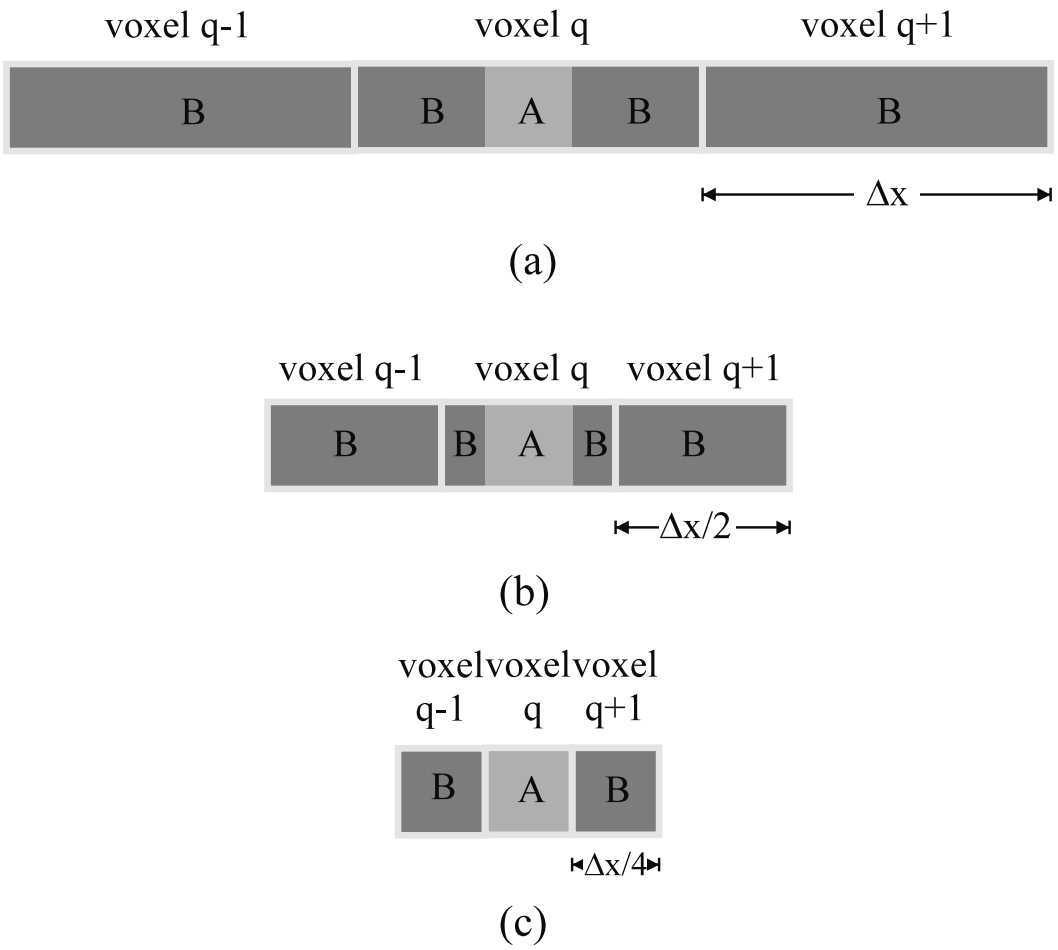

Fig. 15.14: (a) A 1D voxel of dimension Δx contains a square object $\Delta x/4$ in size. The voxel size is reduced to (b) $\Delta x/2$ and (c) $\Delta x/4$ to demonstrate the potential effects of partial voluming. For case 1, the actual CNR between tissues from (a) to (c) increases by a factor of 2 (as discussed in Sec. 15.6). This can also be understood by considering the change in voxel signal for A when B is zero. For part (a), the signal in voxel q will appear as $S_A/4$ and remain at this value for parts (b) and (c) while the noise decreases by $\sqrt{2}$ at each step.

Let ρ_m in the absence of noise be a. If the noise-free phase is $\hat{\phi}$ then the real and imaginary parts, R and I, respectively, of $\hat{\rho}$ are

$$R = a\cos\hat{\phi} + \eta_1 \tag{15.74}$$
$$I = a\sin\hat{\phi} + \eta_2 \tag{15.75}$$

where R and I are the real and imaginary parts of the reconstructed complex voxel signal, respectively, and η_1 and η_2 are noise samples from a Gaussian distribution with mean zero and variance σ^2. The mean values of R and I, $\bar{R}$ and $\bar{I}$, respectively, are

$$\bar{R} = a\cos\hat{\phi} \tag{15.76}$$
$$\bar{I} = a\sin\hat{\phi} \tag{15.77}$$

Their variances are both equal to σ^2. The magnitude ρ_m of the voxel signal is found from

$$\begin{aligned}\rho_m &= (R^2 + I^2)^{1/2} \\ &= (a^2 + 2\eta_2 a\cos\hat{\phi} + 2\eta_1 a\sin\hat{\phi} + \eta_1^2 + \eta_2^2)^{1/2} \\ &\simeq a\left(1 + \frac{\eta_2}{a}\cos\hat{\phi} + \frac{\eta_1}{a}\sin\hat{\phi}\right)\end{aligned} \tag{15.78}$$

With the approximation made for ρ_m in (15.78), the mean of the magnitude of the voxel signal is, as expected, given by

$$\overline{\rho_m} = a \tag{15.79}$$

To obtain the variance of the magnitude, the noise is taken to be uncorrelated between the real and imaginary channels. Then, from (15.78),

$$\begin{aligned}\mathrm{var}(\rho_m) &\equiv \sigma^2_{\mathrm{mag}} \\ &= \mathrm{var}(\eta_2)\cos^2\hat{\phi} + \mathrm{var}(\eta_1)\sin^2\hat{\phi} \\ &= \sigma^2\end{aligned} \tag{15.80}$$

i.e., if the SNR of the magnitude of the voxel signal is much larger than unity, the mean of the magnitude is the true magnitude value, and its variance is the same as the variance in either the real or imaginary part of the voxel signal.

Problem 15.14

An alternate approach can be taken to obtain (15.79) and (15.80) for the case of large SNR. In this limit, the added white noise can be approximated as producing a small error in the measurement of the true magnitude ($\overline{\rho_m}$).

1) The measured voxel signal magnitude ρ_m can then be expanded in a Taylor series around the value $\overline{\rho_m}$ by viewing ρ_m as a function of R and I, the real and imaginary parts of the voxel signal, respectively. With the SNR large, the approximation of its Taylor series up to the linear term is good enough. Using this approximation, write an expression for the error in the measured magnitude, $\delta\rho_m \equiv \rho_m - \overline{\rho_m}$, in terms of the errors in R and I.
2) What is the mean value of $\delta\rho_m$? Assume that $\overline{\delta I} = \overline{\delta R} = 0$.
3) What is the error variance $\overline{(\delta\rho_m - \overline{\delta\rho_m})^2}$? Do you obtain the same result as in (15.80)?

15.7.2 Phase Image SNR

The phase of the signal can be found from

$$\tan\hat{\phi} = I/R \tag{15.81}$$

Using the approach of differentials on (15.81) to determine the error as in Prob. 15.14 gives

$$\delta\hat{\phi}\sec^2\hat{\phi} = \frac{\delta I}{R} - \delta R\frac{I}{R^2} \tag{15.82}$$

Hence, $\overline{\delta\hat{\phi}} = 0$ and the variance of the phase is given by the mean squared error:

$$\begin{aligned}\overline{\delta\hat{\phi}^2} &= \left(\frac{I}{R}\right)^2\left(\frac{\overline{\delta I^2}}{I^2} + \frac{\overline{\delta R^2}}{R^2}\right)\cos^4\hat{\phi} \\ &= \sigma^2\cos^4\hat{\phi}\left(\frac{\rho_m^2}{R^4}\right) \\ &= \frac{\sigma^2}{\rho_m^2}\end{aligned} \tag{15.83}$$

and the standard deviation of the phase $\sigma_{\text{phase}} \simeq (\overline{\delta\hat{\phi}^2})^{1/2} = \sigma/\rho_m$. This is sometimes written as

$$\sigma_{\text{phase}} = 1/\text{SNR}_{\text{mag}} \quad \text{(units are radians)} \tag{15.84}$$

or in degrees as

$$\sigma_{\text{phase}} = \frac{180^\circ}{\pi(\text{SNR}_{\text{mag}})} \tag{15.85}$$

where SNR_{mag} is the SNR of the voxel signal magnitude. This tells us that at voxels where the SNR of the magnitude is very high, there is a relatively low error in phase measurements. On the other hand, the error is very large if the voxel magnitude has very low SNR.

One of the interesting features of the phase is that if there are artifacts which are of very low magnitude in comparison with the object signal (such as ghosts), the magnitude image does not show these features well. However, these artifacts still have some nonzero phase and even the smallest magnitude effects are highlighted. Such an example is shown in Fig. 15.15.

15.8 SNR as a Function of Field Strength

Finding the optimal field strength for imaging has always been complicated and controversial since many factors affect the outcome. Perhaps the three most important are spin density, T_1, and field inhomogeneity, all of which lead to modifications of SNR and CNR as a function of field strength.

In this section, we will give a prediction of the signal as a function of field strength based on (15.9) and (15.87) and a practical estimate of the ratio of the significance of the two terms in (15.87) at one field strength (the two terms being formed by bulking together the coil and electronics resistances as the sum of electronic resistance R_{coil}, $R_{electronics}$, and the magnetically induced losses due to the presence of the body, R_{body}).

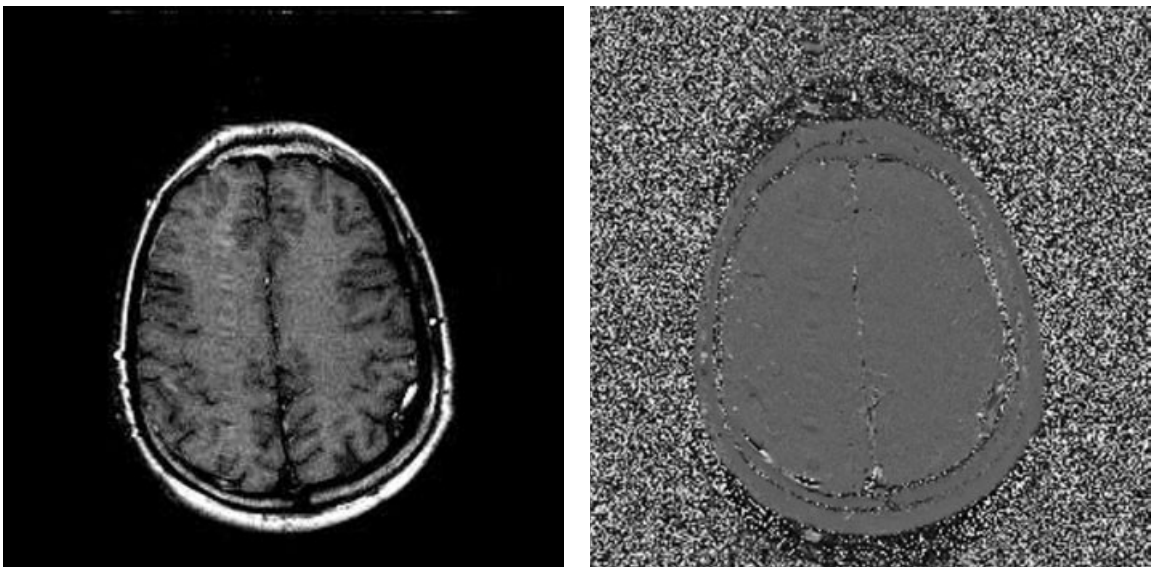

(a) (b)

Fig. 15.15: Low amplitude features such as ghosts are typically highlighted in the phase image. Although a shifted ghost is present in the phase encoding direction, (a) it does not show on the magnitude image, yet, it is well depicted in (b) the phase image.

15.8.1 Frequency Dependence of the Noise in MRI

It was observed in Ch. 7 that the induced emf is proportional to $\omega_0 M_0$. Since $M_0 \propto \omega_0$ too, the induced emf increases as the square of the field strength. In a circuit with a frequency-independent resistance, the rms noise voltage is also independent of the frequency (from (15.7)), depending only on the bandwidth of data collection. Unfortunately in MR, the effective resistance 'seen' by the signal-receiving electronics is found to depend on the operating frequency. This dependence causes the rms noise voltage to be frequency-dependent. The resistance of the coil and the electronics can be bulked together as one component contributing to the noise, while the sample resistance corresponds to the other major contributor to the noise voltage. At low frequencies, the coil and electronics resistance dominate over the sample resistance at room temperatures, whereas at high frequencies, the sample resistance of human tissues dominates the coil and electronics resistance.

Let $\omega_{0,mid}$ be some frequency where this transition of noise source dominance begins to occur:

$$R_{eff}(\omega_0) \approx \begin{cases} R_{coil}(\omega_0) + R_{electronics}(\omega_0) & \omega_0 \ll \omega_{0,mid} \\ R_{sample}(\omega_0) & \omega_0 \gg \omega_{0,mid} \end{cases} \tag{15.86}$$

It has been found that the combined coil and electronics resistances have a square-root dependence on ω_0, whereas the sample resistance has an ω_0^2 dependence, i.e.,

$$R_{eff}(\omega_0) \propto \begin{cases} \sqrt{\omega_0} & \omega_0 \ll \omega_{0,mid} \\ \omega_0^2 & \omega_0 \gg \omega_{0,mid} \end{cases} \tag{15.87}$$

and, from (15.7)

$$\sigma_{thermal} \propto \begin{cases} \omega_0^{1/4} & \omega_0 \ll \omega_{0,mid} \\ \omega_0 & \omega_0 \gg \omega_{0,mid} \end{cases} \tag{15.88}$$

since $\sigma^2_{thermal} \propto R_{eff}$. As a result, when the experiment is designed such that the noise is white noise dominated, the SNR as a function of frequency ω_0 is such that

$$\mathrm{SNR}(\omega_0) \propto \begin{cases} \omega_0^2/\omega_0^{1/4} = \omega_0^{7/4} & \omega_0 \ll \omega_{0,mid} \\ \omega_0^2/\omega_0 = \omega_0 & \omega_0 \gg \omega_{0,mid} \end{cases} \tag{15.89}$$

i.e., at low field strengths, a 7/4 power law improvement in SNR with field strength occurs, whereas at high field strengths, only a linear increase in SNR is obtained. The practical implications of this frequency dependence will be discussed in more detail in Sec. 15.8.2. It suffices to say here that the SNR increases not as ω_0^2 as it would have if $\sigma_{thermal}$ were frequency-independent. It increases only as $\omega_0^{7/4}$ until some transition frequency, after which it increases further slowly for $\omega_0 \gg \omega_{0,mid}$. It is also worth reminding the reader here that at a given frequency, the rms noise voltage depends on the measurement bandwidth BW_{read}.

15.8.2 SNR Dependence on Field Strength

We start with a low field system ($B_{0,low} = 0.065\,\mathrm{T}$), where one expects the noise to be dominated by the electronics. In this case, using a high temperature superconducting surface coil, it has been shown that the noise is reduced by a factor of 2 compared to a conventional coil at room temperature. If one assumes that the remaining noise is from magnetic losses, then it is possible to calculate the ratio of R_{body} to $R_{electronics}$ and predict the SNR increase from 0.065 T to a high field such as 1.5 T, for example. Using the above information in the generalized expression for SNR given the field dependence of R_{eff} in (15.87),

$$\mathrm{SNR}(\omega) = \kappa \frac{\omega^2}{(\omega^2 + a\sqrt{\omega})^{1/2}} \tag{15.90}$$

implies $a = 3\omega_{low}^{3/2}$ where here $\omega_{low}/\gamma = B_{0,low}$ and $\omega = \gamma B_0$ (for simplicity the subscript 0 used in the previous subsection is dropped from ω at this point). The constant κ contains the system scale factor Λ and all other terms on which signal depends. Using the fact that the noise is reduced by a factor of 2, as mentioned above, yields

$$\mathrm{SNR}(\omega) = \mathrm{SNR}(\omega_{low}) \left[\frac{\left(\frac{\omega}{\omega_{low}}\right)^2}{\left(\left(\frac{\omega}{\omega_{low}}\right)^2 + 3\sqrt{\frac{\omega}{\omega_{low}}}\right)^{1/2}} \right] \tag{15.91}$$

Figure 15.16 demonstrates that above 0.5 T, the SNR is linear in ω to within 6.3% of the predicted value and, below 0.04 T, it is proportional to $\omega^{7/4}$ within 37%.

Implications for Low Field Strength Imaging

The possibility of imaging at low fields appears rather dismal from these predictions assuming that the imaging parameters at 1.5 T are ideal. However, at lower fields both T_1 and

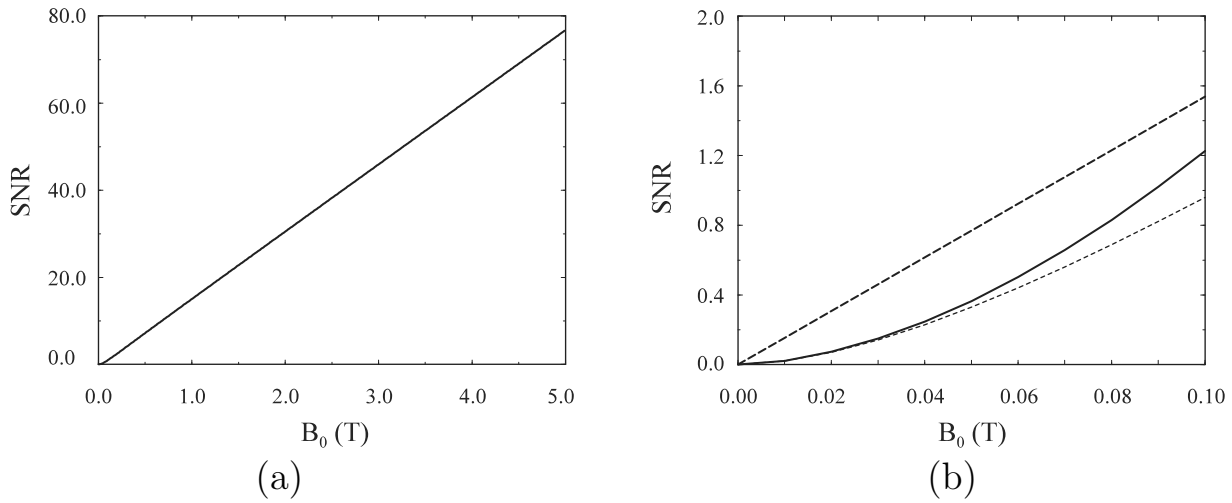

Fig. 15.16: Plot of SNR as a function of field strength. (a) Overall dependence shown over a range of 0.001 T to 5.0 T. (b) Comparison of the dependence with the 7/4 power law (shown as the curve with the short dashed line) and linear behavior (long-dashed line) over a range of 0.001 T to 0.1 T.

susceptibility effects are reduced. For example, it has been empirically shown that

$$T_1(\omega) = 1/(A/\sqrt{\omega} + B) \tag{15.92}$$

This inverse square-root dependence of the longitudinal relaxation rate on the field strength was observed by Escanyé in the article cited in the Suggested Reading found at the end of the chapter. For the tissues evaluated, B was found to be very close to zero, i.e., the relaxation rate was found to vary inversely as the field strength. Recall that for spin echo or gradient echo imaging for short T_R, the signal is proportional to T_R/T_1 so a $\sqrt{\omega}$ decrease in T_1 leads to a $\sqrt{\omega}$ increase in signal.

Problem 15.15

Another estimate for the field dependence of tissue T_1 is

$$T_1(\omega) = a\omega^b \tag{15.93}$$

This power law dependence of T_1 on field strength was proposed by Bottomley in the article cited at the end of this chapter. For gray matter, the values of a and b were found to be 0.00362 and 0.3082, respectively; for white matter, the values are 0.00152 and 0.3477, respectively. For (15.93), plot $T_1(\omega)$ from 1 MHz to 200 MHz for GM and WM. Note that in comparison with the square-root increase in T_1 with field strength described in the text, this predicts approximately a cube root increase in T_1 with field strength. What effects do you expect to see for T_1-weighted scans as the field changes from 1.5 T to 3.0 T?

Also at lower fields, as long as $T_s/2$ is much shorter than T_E at 1.5 T, BW_{read} for a fixed Δx can be reduced proportional to field strength thanks to lower susceptibilities at lower fields and hence reduced signal dephasing and image distortion artifacts. Therefore, down to some field strength where the limiting case is reached, SNR goes up by another factor of $\sqrt{\omega}$. Lo and behold, dependence on ω from the previous SNR argument, under some circumstances, is exactly balanced by the opposite dependence on ω from the two arguments just described.

Problem 15.16

At high magnetic fields, R_2^* of blood becomes a function of field strength. Assume that R_2^* varies directly with magnetic field. Show that the SNR would vary as $\sqrt{B_0}e^{-\alpha T_E B_0}$ for a fixed echo time if the readout bandwidth is also increased to avoid further geometric distortion as B_0 increases. Comment on an optimal choice of B_0 under these conditions.

Suggested Reading

Basic concepts of noise are well described in the following two books:

- C. Kittel. *Thermal Physics*. John Wiley and Sons, Inc., New York, 1969.
- H. L. Van Trees. *Detection, Estimation, and Modulation Theory. Part I*. John Wiley and Sons, Inc., New York, 1968.

The concepts of visibility and detectability are introduced in:

- A. Rose. *Vision: Human and Electronic*. Plenum Press, New York, 1985.

A measure of imaging efficiency is proposed in:

- W. A. Edelstein, G. H. Glover, C. J. Hardy and R. W. Redington. The intrinsic signal-to-noise ratio in NMR imaging. *Magn. Reson. Med.*, 3: 604, 1986.

Issues of contrast and visibility in MR imaging are covered in the following two papers:

- R. T. Constable and R. M. Henkelman. Contrast, resolution, and detectability in MR imaging. *J. Comput. Assist. Tomogr.*, 15: 297, 1991.
- R. Venkatesan and E. M. Haacke. Role of high resolution in magnetic resonance (MR) imaging: Applications to MR angiography, intracranial T_1-weighted imaging, and image interpolation. *Int. J. Imaging Sys. Technol.*, 8: 529, 1997.

The square-root field strength dependence of T_1 was proposed in:

- J. M. Escanyé, D. Canet and J. Robert. Frequency dependence of water proton longitudinal nuclear magnetic relaxation times in mouse tissues at 20°C. *Biochim. Biophys. Acta*, 721: 305, 1982.

The cube root field strength dependence suggested in Prob. 15.15 was observed in:

- P. A. Bottomley, C. J. Hardy, R. E. Argersinger and G. Allen-Moore. A review of ^{1}H nuclear magnetic resonance relaxation in pathology: Are T_1 and T_2 diagnostic? *Med. Phys.*, 14: 1, 1987.